University of Alberta

Finite Element Micromechanical Modeling of Glass Fiber/epoxy Cross-ply Laminates

By

Yu Chen ©

A thesis submitted to the Faculty of Graduate Studies and Research in partial fulfillment of the requirements for the degree of Master of Science

Department of Mechanical Engineering

Edmonton, Alberta

Spring, 2000

National Library of Canada
Acquisitions and Bibliographic Services
395 Wellington Street
Ottawa ON K1A 0N4
Canada

Bibliothèque nationale du Canada
Acquisitions et services bibliographiques
395, rue Wellington
Ottawa ON K1A 0N4
Canada

Your file Votre référence

Our file Notre référence

The author has granted a non-exclusive licence allowing the National Library of Canada to reproduce, loan, distribute or sell copies of this thesis in microform, paper or electronic formats.

L'auteur a accordé une licence non exclusive permettant à la Bibliothèque nationale du Canada de reproduire, prêter, distribuer ou vendre des copies de cette thèse sous la forme de microfiche/film, de reproduction sur papier ou sur format électronique.

The author retains ownership of the copyright in this thesis. Neither the thesis nor substantial extracts from it may be printed or otherwise reproduced without the author's permission.

L'auteur conserve la propriété du droit d'auteur qui protège cette thèse. Ni la thèse ni des extraits substantiels de celle-ci ne doivent être imprimés ou autrement reproduits sans son autorisation.

0-612-60110-2

Canada

University of Alberta

Library Release Form

Name of Author: Yu Chen
Title of Thesis: Finite Element Micromechanical Modeling of Glass Fiber/epoxy Cross-ply Laminates
Degree: Master of Science
Year this Degree Granted: 2000

Permission is hereby granted to the University of Alberta Library to reproduce single copies of this thesis and lend or sell such copies for private, scholarly, or scientific research purposes only.

The author reserves all other publication and other rights in association with the copyright in the thesis, and except as herein before provided, neither the thesis nor any substantial portion thereof may be printed or otherwise reproduced in any material from whatever without the author's prior written permission.

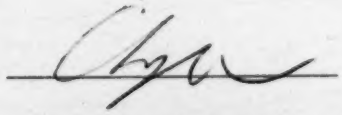

Rm. 102, 10837-86 Ave.
Edmonton, Alberta, T6E 2N1
Canada

11-29-1999

University of Alberta

Faculty of Graduate Studies and Research

The undersigned certify that they have read, and recommended to the Faculty of Graduate Studies and Research for acceptance, a thesis entitled Finite Element Micromechanical Modeling of Glass Fiber/epoxy Cross-ply Laminates submitted by Yu Chen in partial fulfillment of the requirements for the degree of Master of Science.

Fernand Ellyin

Zihui Xia

Dave Chan

Ken Fyfe

99-11-26

Abstract

The focus of this study was to develop the micromechanical model associated with proper damage model to predict the overall mechanical behavior of glass fiber/epoxy cross-ply laminates as well as the damage initiation and propagation inside the laminates. The micromechanical models involved modeling a $[0,90]_{ns}$ laminate that has the periodicity in all directions, and a $[0,90_3,0]_T$ laminate that has no periodicity in thickness direction. The analysis of two different models was all carried out through the finite element method. The epoxy matrix is represented by a nonlinear viscoelastic model. The prediction of overall stress-strain response and the damage initiation and propagation of the $[0,90_3,0]_T$ laminate was conducted through the micromechanical model. The thermal residual stress evolution in the $[0,90]_{ns}$ laminate and the free edge effects on the damage initiation of the $[0,90]_{ns}$ laminate were also investigated through the micromechanical model.

Table of Contents

1. Introduction 1

1.1Macromechanical Approach 2

1.2 Micromechanical Approach 4

1.3 Overview of the current study 9

Bibliography 11

2. A Meso/Micro-mechanical Modeling and Damage Progression of Glass Fiber/Epoxy Cross-Ply Laminates by Finite Element Analysis 15

2.1 Introduction 15

2.2 Development of representative volume element 17

2.2.1. Finite element modeling & boundary conditions 19

2.2.2 Material models for the fiber and epoxy matrix 20

2.3 Damage criterion for epoxy matrix and implementation of damage process in FEM analysis 23

2.4 Numerical results and comparison with experiments 25

2.5 Conclusions 27

Figures — Chapter 2 28

Bibliography 36

3. Finite Element Mircromechanical Modeling of Free Edge Effects in Glass Fiber/Epoxy Cross-ply Laminates 38

3.1 Introduction 38

3.2. Micromechanical modeling approach 40

3.2.1. Finite element modeling of free edge surface 41

3.2.2 Applied boundary conditions 42

3.3 Materials model for the fiber and epoxy matrix 43

3.4 Modeling damage initiation and propagation in finite element analysis 45

3.5 Results and discussion 48

3.6 Conclusions 50

Figures — Chapter 3 52
Bibliography 59

4. A Viscoelastic Micro-mechanical Analysis of Thermal Residual Stress Evolution in Glass Fiber/Epoxy Cross-ply Laminates **62**
4.1 Introduction 62
4.2 Micromechanical modeling 64
4.2.1 Finite element representation 64
4.2.2 Applied boundary conditions 65
4.2.3. Material models for the fiber and epoxy matrix 66
4.2.4. Implementation of thermal analysis in the model 68
4.3 Results and Discussion 69
4.3.1 Residual stresses in fiber/epoxy laminates 69
4.3.2 Free Surface effect on residual stress of cross-ply laminate 70
4.3.3 Stress relaxation of the cross-ply laminate 71
4.3.4. Time effect on thermal expansion coefficient of viscoelastic composites 73
4.4 Conclusions 76
Figures — Chapter 4 77
Bibliography 87

5. Conclusions **89**

List of Figures

Figure 2.1	Representative Volume Element for $[0/90_3/0]_T$ laminate.	28
Figure 2.2	Three-dimensional finite element mesh for RVE of $[0/90_3/0]_T$ laminate.	29
Figure 2.3	A viscoelastic model represented by a finite series of Kelvin elements coupled with an elastic spring.	30
Figure 2.4	Stress-strain curves of epoxy under uniaxial tests with different stress rates.	30
Figure 2.5	A stress relaxation test result and model prediction for epoxy matrix.	31
Figure 2.6	Stress-strain curve of epoxy with damage criterion.	32
Figure 2.7	FEM Predicted stress-strain curves of $[0/90_3/0]_T$ laminate with and without damage analysis.	32
Figure 2.8	Stress distribution of σ_{xx} component at the applied global strain value of 0.58%.	33
Figure 2.9	Maximum principal strain distribution at the applied global strain value of 0.58%.	33
Figure 2.10	Damage growth in the RVE model.	34
Figure 2.11	Damage growth in the RVE model by elastic solution with damage criterion.	35
Figure 3.1	Micromechanical Representation of an interior element of $[0/90]_{ns}$ cross-ply laminate.	52
Figure 3.2	A representative micromechanical model near free edge surface for $[0/90]_{ns}$ laminate.	52
Figure 3.3	Three-dimensional finite element mesh of micromechanical model near free edge surface for $[0/90]_{ns}$ laminate.	53
Figure 3.4	A viscoelastic model represented by a finite series of Kelvin elements coupled with an elastic spring.	54
Figure 3.5	Stress-strain response of an epoxy matrix element with the damage criterion of the maximum principle strain.	54

Figure 3.6	Maximum principal strain distribution at the applied global strain value of 0.52% by two different models.	55
Figure 3.7	Prediction of damage initiation by the free edge model.	56
Figure 3.8	Prediction of damage propagation by the free edge model.	57
Figure 3.9	Prediction of damage propagation by the interior RVE model.	58
Figure 3.10	Prediction of stress-strain response of $[0/90]_{ns}$ laminate by the interior RVE model.	59
Figure 4.1	Representative Volume Element for [0/90] laminate.	77
Figure 4.2	A RVE model near free edge surface for [0/90] laminate.	77
Figure 4.3	The 3-D models and FEM meshing.	78
Figure 4.4	A viscoelastic model represented by a finite series of Kelvin elements coupled with an elastic spring.	79
Figure 4.5	Residual stress distribution for unidirectional laminate at cooling rate of 1.4° C/min.	80
Figure 4.6	Residual stress distribution for cross-ply laminate at cooling rate of 1.4° C/min.	81
Figure 4.7	Thermal residual stresses distributions in longitudinal direction (σ_{zz}) for cross-ply laminate near and away from free edge surface at cooling rate of 126° C/min.	82
Figure 4.8	Thermal residual stresses distributions in longitudinal direction (σ_{zz}) for cross-ply laminate with two different matrix materials.	83
Figure 4.9	Residual stresses distribution for cross-ply laminate after holding the model at room temperature for 2133 minutes.	84
Figure 4.10	Residual stress relaxation in cross-ply model for different cooling rates.	85
Figure 4.11	Strain recovery in cross-ply laminate for different cooling rates.	85
Figure 4.12	Calculated average CTE of unidirectional composite.	86
Figure 4.13	Calculated average CTE of cross-ply laminate as a function of time.	87

Chapter 1

Introduction

There has been a considerable increase in the use of advanced composite materials in various industries in recent years. The reason for this increase can be attributed to the great improvement of the stiffness-to-weight ratio and strength-to-weight ratio in composite materials [1]. The development of composite materials with reduced weight and increased strength relative to the conventional metals or alloys, has played a critical role in achieving higher operating performance, long-life and reduced costs. One such composites system is fiber reinforced composite laminates.

These properties of composites, e.g. strength and stiffness, are dependent on the volume fraction of the fibers, and the individual properties of the constituent materials, i.e., the fiber and matrix. In addition, the variation of lay-up configurations of composite laminates allows the designer greater flexibility when incorporating composites into a structure. With this flexibility, however, comes complexity in analysis of composite structures. Particularly, the damage and failure progression in laminated composites is very complicated compared to that of conventional metallic materials. The stiffness and strength in composite structures may vary due to the damage initiation and propagation. The damage modes are matrix cracking, interface debonding and delamination during the loading history of the composite life. Consequently, the modeling of composite materials is more complex than that of traditional engineering materials.

1.1 Macromechanical Approach

Generally, the modeling of composite laminates can be investigated from two distinct levels: macromechanical and micromechanical scales. The macromechanical approach is concerned with the contributions of each ply to the overall properties. It treats each layer as a homogenous, orthotropic, elastic or elastic-plastic continuum [2-3], in which the properties of the fiber and matrix are averaged to produce a set of homogenous, orthotropic properties. Based on the known properties of the individual layers, the macromechanical modeling involves investigation of the interaction of the individual layers of the laminate and their effect on the overall response of the laminate. For a given stacking sequence, the stress-strain relations of a composite laminate can be derived, and the various coupling mechanisms between in-plane and out of plane deformation modes of a composite laminate can be explored.

Classical laminate theory (CLT) [4] is a widely accepted macromechanical approach for the determination of the mechanical behavior of composite laminates. The CLT can be used to predict the overall response of a laminate if the individual plies are linear-elastic. For laminates where individual plies exhibit inelastic response, additional terms are required in the CLT formulation [5], which incorporate inelastic strains into the formulation.

In macromechanical modeling, prediction of failure of a unidirectional fiber-reinforced composite is usually accomplished by comparing some functions of the overall stresses or strains to material strength limits. In the case of composite laminates, however, there is an additional level of complication which arises as a result of stacking several layers of composites with different orientation and properties. In some industrial

applications, the first failure of any layer is not allowed because it degrades the strength and stiffness of the laminate. A prediction based on the first ply failure is commonly referred to as the *first-ply failure criterion* [6]. Several failure criteria such as maximum stress, maximum strain, Tsai-Hill, Tsai-Wu criteria have been suggested to predict the *first-ply failure*. These criteria, however, are based on the averaged composite stress/strain states. Macromechanical modeling does not consider the distinctive behavior of the fiber and matrix materials.

Although the macromechanical approach has the advantage of simplicity, it is not possible to identify the stress/strain states in the fiber, matrix and their interface. In contrast, in the micromechanical approach, the constituents, i.e. the fiber, matrix and their interface, are distinctively considered to predict the overall response of the composite as well as the damage initiation and propagation in the composite. This approach provides more physical information at the fiber and matrix level. This is important for the understanding of damage mechanisms and in predicting damage progression inside the composite laminates. Moreover, the micromechanical approach can predict the effective properties of composite material from the knowledge of the individual constituents. This allows the designers to computationally combine different material properties to determine a particular combination that best meets the specific needs. Consequently, more and more contributions are being presented dealing with the micromechanical modeling.

1.2 Micromechanical Approach

Micromechanical methods have been used in analyzing fiber reinforced composite for more than 20 years. With the ever increasing computing capabilities, more and more detailed micromechanical analyses are being preformed. This approach assumes that the complex microstructure of the composite can be replaced by a representative volume element (RVE) or unit cell. The RVE has a regularly spaced array of parallel cylindrical fibers embedded in the homogeneous matrix material of infinite dimensions so that it can be isolated from the whole structure of the composite. The RVE has the same fiber volume fraction as the composite laminate and the respective properties of the fiber and matrix can be characterized individually. The individual constituents can then be used together in the RVE model such that the overall response of the composite can be predicted.

Previous micromechanical modeling concerned with continuous fiber reinforced composites could be classified into two major groups. One is the analytical method and the other is finite element method. The purpose of this chapter is to review the application of finite element micromechanical modeling to fiber-reinforced composites. For completeness, some representative analytical models are also briefly summarized.

One of the early and simplest analytical models is the vanishing fiber diameter (VFD) model, developed by Dovorak and Bahei-El-Din [7-8]. The model consists of a continuum matrix reinforced by cylindrical fibers of vanishingly small diameter. It is closely aligned with the rule of mixtures but with the additional assumption that the diameter of the fiber is vanishingly small, while still maintaining the finite volume fraction. Consequently, the fiber does not interfere with matrix deformation in the

transverse direction, and only the longitudinal constraint between the fiber and matrix is considered.

A second popular analytical model which has been applied to inelastic matrix composite micromechanics is the self-consistent method [9], which is based on the Eshelby solution of an ellipsoidal inclusion embedded in an infinite matrix subjected to uniform boundary conditions. This method is widely applied in the particle-reinforced composites, however, inelastic analysis has also been performed for the evaluation of the effective properties of fiber-reinforced composites. [10].

Aboudi [11-13] developed a micromechanical analytical model to compute effective moduli of a composite made of nonlinear constituents, and extended the model to predict the strength and fatigue failure of composites. This model was based on a representative unit cell of rectangular shape. The unit cell consisted of four subcells and the fiber cross-section also had a rectangular shape, which was assumed in order to reduce the complexity of the analysis. His model included a variety of effects such as viscoplasticity, residual stress, debonding and creep. The development of this micromechanical model was very elaborate, and involved advanced mathematics.

After the development of unit cell method, great effort has been expanded to study the damage and failure of fiber reinforced composites based on the modified Aboudi model [14-16]. An advantage of this analytical model is that it yields explicit expressions for the overall composite behavior as functions of the constituent properties and a full-field stress/strain solution. However, most analytical models are usually restricted to idealized geometry and stress/strain relations to achieve closed-form solutions. It is therefore, difficult to introduce damage analysis and predict damage

progression in these types of models. In contrast, the finite element micromechanical modeling, surmounts most of the shortcomings associated with analytical models. Therefore, a large number of finite element micromechanical solutions have been developed for various fibrous reinforced composite problems.

The early use of the unit cell in the finite element method to predict the mechanical properties of unidirectional composites was undertaken by Adams and coworkers [17-18]. In his generalized plane strain finite element analysis, he used a square array of fibers as the RVE model to perform a non-linear analysis of boron/aluminum subject to transverse tension including the effect of matrix plasticity. A perfect fiber/matrix interface bond was assumed in this model and the effect of residual stresses was not taken into account. Dvorak and coworkers [19-20] developed another RVE model called the periodic hexagonal array (PHA) model, where the fibers are assumed to be periodically distributed throughout the matrix in a topologically hexagonal configuration. However, since Adams suggested that the assumption of a square packing array provides good correlation with experimental data [21], most of finite element micromechanical models are based on the square array RVE model.

The finite element micromechanical modeling appears to be an effective computational procedure to determine residual stresses in the composite. Many researchers [22-25] have applied Adam's model to study the process-induced residual stress in unidirectional metal matrix composites. In these investigations, high residual stresses were shown to exist around the interface region, hence, the effect of residual stresses became a major concern in the finite element micromechanical modeling of metal matrix composites. It was Bigelow [26] who first extended the micromechanical

analysis to a cross-ply laminate. He developed a three-dimensional finite element RVE model to represent the structure of the cross-ply laminate and study the thermal residual stress in the Silicon-Carbide/Titanium [0/90] laminate. Since this work, the finite element micromechanical modeling has been applied to study cross-ply laminates by other researchers [27-29]. The use of RVE in finite element method has now become an effective method in determining the residual stresses in the composite laminates.

With the increasing computing capabilities, the use of the RVE or unit cell, in the finite element method has become a common numerical tool to investigate damage progression in composites on the microscale. Unlike the macromechanical approach, in which the damage and failure of composites are examined based on the average composite stresses and strains, the damage analysis in micromechanical approach is based on the detailed distribution of stress and strain in the matrix and fiber. With a proper damage criterion, the location where damage is initiates can be easily determined by finite element modeling. Furthermore, the damage evolution process as the applied load increases can also be modeled by the finite element analysis.

Currently, this technique has been widely used in the fiber-reinforced metal matrix composites. In metal matrix composites, the fiber/matrix interfacial damage is a dominant contributor to the inelastic response of the composites. Wisnom [30] has developed an interface element to simulate the interface debonding process in his micromechanical model of a unidirectional composite. A quadratic interaction criterion was assumed between tensile and shear stress for this kind of element:

$$\left(\frac{\sigma}{\sigma_f}\right)^2+\left(\frac{\tau}{\tau_f}\right)^2=1 \qquad (1.1)$$

where σ and τ are the normal and tangential stresses across the interface element and σ_f and τ_f are the failure stresses of interface under tension and shear alone. This criterion has been found to predict reasonably well the failure of composites at the macromechanical level [31]. However, it is very difficult to measure interface strengths experimentally. The failure values selected in his investigation were based on his previous numerical research. Different interface failure criteria as well as different methods to model the interface debonding effect have also been developed by the others [32-33], and include the rate dependent viscoplasticity model for the matrix. Sherwood and Quimby [34] extended the damage analysis of micromechanical modeling in the cross-ply laminate. The effects of perfect and imperfect fiber-matrix interfaces and the rate-dependent matrix behavior on the response of overall properties were investigated through the RVE model representing $[0/90]_{2s}$ metal matrix composites. The weak bond interface was modeled using contact elements in the finite element analysis.

Although matrix cracking is a common damage type in a fiber reinforced composite, only a few investigations [35-37] have been reported with respect to the transverse cracking in the fiber-reinforced composites using the finite element micromechanical model. Talreja and his coworkers [37] have developed three different RVE models (square, hexagonal and square-diagonal) to predict the transverse matrix-initiated failure in unidirectional polymer composites. Two different failure criteria have been induced in the model to predict failure initiation in the matrix. Compared to numerous micromechanical models of interface effects in composites, their models focused on the failure of matrix in composites. However, in this study, both the matrix

and fiber are assumed to be linearly elastic and damage propagation within the composite was not considered in the analysis.

In the past ten years, a considerable amount of work has been done on the micromechanical analysis of elastic and elastic-plastic behavior of composites. The use of micromechanics in the study of mechanical behavior of viscoelastic polymer composites has not been so widespread. The limited applications of micromechanical model in this area have been concerned only with the creep response of unidirectional composites [38-39]. Little work has been reported on the modeling of the matrix cracking in the presence of the viscoelastic matrix for glass fiber/epoxy cross-ply laminates. In addition, in the previous micromechanical models the RVE or unit cell is representative of a typical internal section of the composite that is not influenced by edge effects. To the best of our knowledge, no micromechanical modeling has been carried out on the free edge effects in glass fiber/epoxy cross-ply laminates. Therefore, the main objective of this study is to develop a micromechanical model for the glass fiber/epoxy cross-ply laminates that account for damage evolution and matrix viscoelasticity. The free edge effects and evolution of residual stresses in the cross-ply laminates will also be investigated through micromechanical modeling.

1.3 Overview of the Current Study

In the present work, the finite element micromechanical analysis incorporating the damage criteria is conducted to investigate the behavior of glass fiber/epoxy cross-ply laminates under thermal and mechanical loadings. An important consideration in the current study is to develop a comprehensive RVE model that can provide an accurate

stress/strain state in the fiber and matrix level as well as to allow for a damage analysis in the RVE model of the cross-ply laminate. The micromechanical analysis is conducted as follows:

First, A three-dimensional multi-cell meso/micro-mechanical finite element model has been developed to predict the overall mechanical behavior of a $[0,90_3,0]_T$ glass fiber/epoxy laminate. This model assumes periodic structure in the laminate plane but there is no periodicity in the thickness direction. A damage criterion for the epoxy matrix is introduced into the finite element model. Numerical results from the finite element analysis are compared with the experimental data. It is found that not only the predicted overall stress-strain response but also the prediction of initiation and propagation of the damage are in good agreement with the experimental results.

Second, the free edge effects in a $[0/90]_{ns}$ glass fiber/epoxy cross-ply laminate subjected to mechanical loads are investigated using the finite element micromechanical model. Here, the periodic structure is assumed to extend in all three directions for the interior RVE, but not for that of free edge. Two different damage criteria, one for the matrix cracking and the other for the interface debonding have been introduced into the model and were incorporated into the finite element analysis program, ADINA, through the user-defined subroutine. Based on these two criteria, damage initiation as well as damage propagation in the cross-ply laminate is predicted by the present model. The effect of the free edge on damage initiation and propagation in the cross-ply laminate is compared with that of an interior cell model (periodic structure). It is found that the edge effect is dominant in the damage initiation process, however, its influence on the overall properties of the cross-ply laminate is not significant.

Finally, the effect of viscoelasticity of matrix material on the evolution of processing-induced thermal residual stresses in a $[0/90]_m$ glass fiber/epoxy cross-ply laminate is investigated by the same micromechanical model as in the second part. The finite element thermal stress analysis indicates that a higher cooling rate results in a higher initial residual stress in the laminate. However, the residual stresses do relax with time and tend to an asymptotic small value independent of the cooling rate. The effect of the free edge surface on the generation of residual stresses is also investigated and compared to those of the interior region.

Bibliography

1. Daniel, I.M. and Ishai, O., "Engineering Mechanics of Composite Materials", Oxford University Press, New York, 1994.
2. Hahn, H.T. and Tsai, S.W., "Nonlinear Elastic Behavior of Unidirectional Composite Laminate," *Journal of Composite Materials*, Vol.7, 1973, pp102-118.
3. Sun, C.T. and Chen, J.L., "A simple flow rule for characterizing nonlinear behavior of fiber composites," *Journal of Composite Materials* , Vol. 23, 1989, pp1009-1020
4. Jones, R.M., "Mechanics of Composite Materials", Hemisphere Publishing, New York, 1975.
5. Hiddle, J.S. and Herakovich, C.T. "Inelastic Response of Hybrid Composite Laminates", *Journal of Composite Materials* , Vol. 26, 1992, pp2-9.
6. Tsai, S.W. and Hahn, H.T., " Introduction to Composite Laminates", Technomic Publishing Co., Inc., Lanchaster, PA, 1980.
7. Dvorak, G.J. and Bahei-El-Din, Y.A. "Elastic-Plastic Behavior of Fibrous Composites", *Journal of Mechanics Physics Solids*, Vol.27, 1978, pp51-72.
8. Dvorak, G.J. and Bahei-El-Din, Y.A. "Plasticity Analysis of Fibrous Composite", *Journal of Applied Mechanics*, Vol.49, 1982, pp327-335.

9. Schapery, R. "A Micromechanical Model for Nonlinear Viscoelastic Behavior of Particle-reinforced Rubber with Distributed Damage", *Engineering Fracture Mechanics*, Vol. 25, 1986, pp845-867.

10. Gavazzi, A.C. and Lagoudas, D.C., "On the Numerical Evaluation of Eshelby's Tensor and Its Application to Elastoplastic Fibrous Composites", *Computational Mechanics*, Vol. 7, 1990, pp13-19.

11. Aboudi, J., "Effective Behavior of Inelastic Fiber-reinforced Composites", *International Journal of Engineering Science*, Vol.22, 1984, pp439-449.

12. Aboudi, J., "Micromechanical Analysis of the Strength of Unidirectional Fiber *Composites", Composites Science and Technology*, Vol.33, 1988, pp79-96.

13. Aboudi, J., "Micromechanical Analysis of Composites by the Method of Cells", *Applied Mechanics Review*, Vol.42, 1989, pp193-221.

14. Robertson, D.D. and Mall S, "Micromechanical Analysis of Metal matrix Composite Laminates with Fiber/matrix Interfacial Damage", *Composites Engineering*, Vol. 4, 1994, pp1257-1274.

15. Aidun, J.B. and Addessio, F.L., "Enhanced Cell Model with Nonlinear Elasticity", *Journal of Composite Materials* , Vol. 30, 1996, pp248-280.

16. Kwon, Y.W. and Berner, J.M., "Matrix Damage of Fibrous Composites: Effects of Thermal Residual Stresses and Layer Sequences", *Computers & Structures*, Vol.64, 1997, pp375-382.

17. Adams, D.F. and Crane, D.A., "Finite Element Micromechanical Analysis of a Unidirectional Composite Including Longitudinal Shear Loading", *Computers & Structures*, Vol.18, 1984, pp1153-1165.

18. Adams, D.F. and Crane, D.A., "Combined Loading Micromechanical Analysis of a Unidirectional Composites", *Composites*, Vol.15, 1984, pp181-192.

19. Dvorak, G.J. and Teply, J.L. "Periodic Hexagonal Array Model for Plasticity Analysis of Composite Materials. In Plasticity Today: Modeling, Methods and Application, W. Olszak Memorial Volume, A. Sawxzuk & B.Bianchi (eds.), Elsevier Science Pulishers, Amsterdam, The Netherlands, 1985, pp623-642.

20. Teply, J.L. and Dvorak, G.J., "Bounds on Overall instantaneous properties of elastic plastic composites", *Journal of Mechanics Physics Solids*, Vol.36, 1988, pp29-58.

21. Adams, D.F. and S.W. Tsai. "The influence of Random Filament Packing on the Transverse Stiffness of Unidirectional Composites", *Journal of Composite Materials*, Vol.3, 1969, pp308-318.

22. Nimmer, R.P., Bankert, R. J. and Russel, E.S. "Micromechanical Modeling of Fiber-Matrix Interface Effects in Transversely Loaded SiC/Ti-6-4 Metal Matrix Composites", *Journal of Composites Technology and Research*, Vol.13, 1991, pp3-13.

23. Bigelow, C.A., "The Effect of Uneven Fiber Spacing on Thermal Residual Stresses in a Unidirectional SCS-6/Ti-15-3 Laminate", *Journal of Composites Technology and Research*, Vol.14, 1992, pp211-220.

24. Wisnom, M.R., "Factors Affecting the Transverse Tensile Strength of Unidirectional Continuous Silicon Carbide Fiber Reinforced 6061 Aluminum", *Journal of Composite Materials*, Vol.24, 1990, pp707-726.

25. Chandra, N., Ananth, C.R. and Garmestani, H., "Micromechanical Modeling of Process-Induced Residual Stresses in Ti-24Al-11Nb/SCS-6 Composite", *Journal of Composites Technology and Research*, Vol.16, 1996, pp34-46.

26. Bigelow, C.A., "Thermal Residual Stresses in a Silicon-Carbide/Titanium [0/90] laminate", *Journal of Composites Technology and Research*, Vol.15, 1993, pp304-310.

27. Rangaswamy, P. and Jayaraman, N. "Residual Stresses in SCS-6/Ti-24Al-11Nb Composite: Part II-Finite Element Modeling", *Journal of Composites Technology and Research*, Vol.16, 1994, pp304-310.

28. Dix, B.E., Saigal, A. and Greif, R., "Thermal Stresses in Unidirectional and Cross-ply Composite Laminates: A 3-D Micromechanical Investigation", *Proceedings of the ASME Aerospace Division, Vol.52*, International Mechanical Engineering Congress and Exposition, Atlanta, GA, Nov. 17-22, 1996, pp435-444.

29. W.Zhong, T.H. Lin and S.R. Lin, "An Elastic-plastic Micromechanical Analysis of a Cross-ply Composite", *Composites Science and Technology*, Vol.58, 1998, pp527-537.

30. Wisnom, M.R., "Micromechanical Modeling of the Transverse Tensile Ductility of Unidirectional Silicon Carbide/6061 Aluminum", *Journal of Composites Technology and Research*, Vol.14, 1992, pp61-69.

31. Hashin, Z., "Failure Criteria for Unidirectional Fiber Composites", *Journal of Applied Mechanics*, Vol.47, 1980, pp329-334.

32. Allen, D.H., Jones, R.H. and Boyd, J.G. "Micromechanical Analysis of a Continuous Fiber Metal Matrix Composite Including the Effect of Matrix Viscoplasticity and Evolving Damage", *Journal of Mechanics Physics Solids*, Vol.42, 1994, pp505-529.

33. Lissenden, C.J. and Herakovich, C.T., "Numerical Modeling of Damage Development and Viscoplasticity in Metal Matrix Composites", *Computer Method in Applied Mechanics and Engineering*, Vol.126, 1995, pp289-303.

34. Sherwood, J.A. and Quimby, H.M. "Micromechanical Modeling of Damage Growth in Titanium Based Metal-Matrix Composites", *Computers & Structures*, Vol.56, 1995, pp505-514.

35. Adams, D.F. "Micromechanical Modeling of Yielding and Crack Propagation in unidirectional metal matrix composite", *Testing Technology of Metal Matrix Composites, ASTM STP 964*, American Society for Testing and Materials, Philadelphia, PA, 1988, pp93-103.

36. Kwon, Y.W., "Calculation of effective modulli of fibrous composites with or without micro-mechanical damages", *Composite Structures*, Vol.25, 1993, pp187-192.

37. Asp, L.E., Berglund, L.A., and Talreja, R., "Prediction of Matrix-initiated Transverse Failure in Polymer Composites", *Composites Science and Technology*, Vol.56, 1996, pp1089-1097.

38. Yancey, R.N. and Pindera, M.J., "Micromechanical Analysis of the Creep Response of Unidirectional Composites", *Journal of Engineering Materials and Technology*, Vol. 112, 1990, pp157-163.

39. Wen, Y.F., and Gibson, R.F., "Prediction of Momentary Transverse Creep Behavior of Thermoplastic Polymer Matrix Composites Using Micromechanical Models", *Journal of Composite Materials*, Vol.31, 1997, pp2124-2145.

Chapter 2

A Meso/Micro-mechanical Modeling and Damage Progression of Glass Fiber/Epoxy Cross-Ply Laminates by Finite Element Analysis

2.1 Introduction

Continuous fiber-reinforced polymeric composites have been successfully used in many structural applications due to their lightweight, high specific stiffness and strength. Consequently, it is important to understand as well as to predict the overall mechanical behavior of fiber-reinforced polymeric laminates from their constituent properties.

Generally, two approaches are taken in obtaining the global properties of composites: (a) a macro-mechanical modeling and (b) a micro-mechanical representation. The former utilizes the experimental data from standard coupon specimens to build a constitutive equation [1]; while the latter typically uses the unit cell technique combined with the known material properties of fiber and matrix to determine the overall behavior of composites [2-3]. The macro-mechanical approach treats the composite as a homogeneous orthotropic continuum. The required experimental program to evaluate various material constants and functions in the macroscopic constitutive equation is relatively costly and time-consuming [4]. Furthermore, local damage cannot be predicted by these models. The micro-mechanical method is based on the known properties of the constituents and the assumption that the

composite possesses a periodic structure. Thus, a representative volume element (RVE) or unit cell model is first constructed depending on the geometry and loading condition of the composite. The properties of the composite are then obtained through an analysis of the RVE or unit cell model either by analytical or numerical methods. The overall properties of composites can be predicted quite accurately by a micro-mechanical model as long as the properties of the constituents (fiber and matrix) are properly represented in the model [5-6]. Moreover, it is convenient to carry out parametric studies using the micro-mechanical model. Various mechanisms including damage initiation and propagation, and their influence on the global performance of the composites can also be studied through the micro-mechanical analyses.

Therefore, using a micro-mechanical model to predict the overall composite behavior by means of the constituent properties has distinct advantages. Most analyses [7-10] have used the unit cell micro-mechanical model to study the mechanical properties of *unidirectional* fiber reinforced composites. A few investigators have also applied the micromechanical analysis to the cross-ply metal matrix laminates [11-12]. The current work extends the micro-mechanical analysis to a cross-ply viscoelastic polymer laminate. In this model, the periodic condition is assumed only in in-plane directions, while in thickness direction no periodicity exists. The lay-up structure of a cross-ply laminate is simulated through a multi-layer unit cell model. Hence, the word "meso" is used to distinguish this feature from a fully periodic structure in all three directions.

In this study, the epoxy matrix is represented by a nonlinear viscoelastic constitutive model [13], which was implemented into the finite element analysis code,

ADINA, through a user-defined subroutine. Experiments [14] on the coupon specimen indicate that transverse cracking in the epoxy matrix could start at a relatively low applied load. In order to investigate this mechanism, a damage criterion for the epoxy matrix is introduced. A three-dimensional finite element analysis is conducted on the multi-layer cell model. The numerical results from finite element analysis are compared with the experiment data.

2.2 Development of Representative Volume Element

The micro-mechanical model is set up based on the representative volume element (RVE) technique. It is assumed that fibers are uniformly distributed in matrix and have the same radii. Therefore, each unidirectional layer could be represented by a unit cube with a single fiber having the same fiber volume fraction as the ply. For a cross-ply laminate, if the number of layers in each direction is not the same, then a proper combination of the unit cells can be used to reflect the proportion and the lay-up sequence. It is to be noted that in an actual unidirectional lamina, there might be many fibers randomly dispersed across its thickness. The use of a single unit cube to represent such non-monofilament layer may neglect fiber interaction within a lamina. Thus, in such a case the representation is strictly a "meso" homogenization process for each lamina.

Figure 2.1 shows a meso/micro-mechanical representation of a $[0,90_3,0]_T$ laminate. A feature of this laminate is that no periodical structure exists in the thickness direction. The lay-up structure of the laminate has been represented by stacking the unit cube cells in a proper sequence. Due to the periodicity in the XZ-plane, a representative

volume element thus consists of two cells with 0° fiber and three cells with 90° fiber orientation. This representative structure could be envisaged as a building block of the laminate, as depicted in Fig.2.1. The periodic boundary conditions are imposed only in the XZ plane for the above mentioned representative volume element. It is to be noted that the same RVE can be used if the number of each layer in the laminate is doubled, i.e., $[0_2,90_6,0_2]_T=[0_2,90_3]_S$, provided the original volume fraction for each layer holds. If the applied in-plane load is symmetric with respect to the mid-plane, then symmetry of the boundary conditions and the geometry would allow 1/8 of the multi-cell model to be analyzed as a RVE. In the analysis to follow, the fiber volume fraction was taken to be 52.5%, which is the same for each layer in the laminate.

If the in-plane dimensions of the laminate are much larger than that in the thickness direction, the stress and strain fields in the laminate will be periodic in nature (represented by the RVE model), except near the free edges and near the area where the external load is applied. Therefore, we restrict our attention to the interior domain, i.e. the edge effect is not included. Consequently, the macro-stress and macro-strain of the composite can be represented by averaged stress and averaged strain in the RVE:

$$\sigma_{ij}^{c} = \overline{\sigma_{ij}^{R}} \tag{2.1}$$

$$\varepsilon_{ij}^{c} = \overline{\varepsilon_{ij}^{R}} \tag{2.2}$$

In this study, we will consider a $[0,90_3,0]_T$ laminate under strain-controlled loading. The load is applied along the 0° fiber direction with a constant strain-rate of $10^{-5}s^{-1}$. A residual stress field might be introduced during the manufacturing process of the laminate due to the difference in thermal coefficients of the fiber and the epoxy

matrix. However, a major part of the residual stress in the epoxy matrix material may relax with the passage of time (see the section on material properties, Fig.2.5b). Thus, the effect of residual stress is neglected in the present analysis. Instead of deriving the complex mathematical expression for the averaged stress and strain of the RVE, as demonstrated by e.g. Aboudi [2], and Roberston [15], among others, the finite element analysis will be used to obtain the averaged stress and strain of the RVE.

2.2.1 Finite Element Modeling and Boundary Conditions

The RVE model is meshed with three-dimensional, eight-node hexahedral elements. The finite element mesh is constructed with 3974 nodes and 3204 brick elements, as shown in Fig 2.2. Sufficiently fine elements were used for the matrix part, especially near the fiber/matrix interface, where a significant stress gradient may occur. The viscoelastic numerical results were also obtained through a finer meshed model (about 70% more nodes were used). In comparison with the mesh in Fig.2.2, the finer meshed model results in no appreciable changes in the stress/strain contours and the damage propagation path. Therefore, the model shown in Fig.2.2 is sufficient to obtain convergent results.

Symmetric conditions were applied to the boundary surfaces X=0, Y=0 and Z=0:

$$u(0,Y,Z) = 0 \tag{2.3}$$

$$v(X,0,Z) = 0 \tag{2.4}$$

$$w(X,Y,0) = 0 \tag{2.5}$$

The boundary conditions applied to the surfaces X=1 and Z=1 should enforce periodicity along the X- and Z-directions:

$$u(1, Y, Z) = u(1,0,0) \tag{2.6}$$

$$w(X, Y, 1) = w(0,0,1) \tag{2.7}$$

It is to be noted that, in this investigation, the external load (uniaxial loading case) was applied by prescribing the displacement u(1,0,0). The nodes on plane X=1, were free to displace in the plane but were all constrained to have the same normal displacement u during the deformation in order to maintain a flat surface (see equation (6)). Therefore, the resultant traction on this plane would contain only a normal component. The normal displacement w for all nodes on plane Z=1, is the same, but it is not prescribed. Thus, this surface is allowed to move in the normal direction freely but remains plane (see equation (7)), and therefore, the resultant normal and shear forces in this plane will be equal to zero. Finally, the nodes on the top surface, Y=5, were left free to simulate the free surface condition of the laminate.

Sun [16] has shown that, under the above boundary conditions, the average stress and strain in the RVE can be obtained from:

$$\overline{\varepsilon_{11}^{R}} = \frac{u(1,0,0)}{L} \tag{2.8}$$

$$\overline{\sigma_{11}^{R}} = \frac{P}{A} \tag{2.9}$$

where L is the length of model in X direction, P is the sum of reactions at nodes on the surface X=1 and A is the area of that surface, and subscript 1 refers to X-direction.

2.2.2 Material Models for the Fiber and Epoxy Matrix

The E-glass fiber was assumed to remain linearly elastic, and thus was modeled through a generalized Hooke's law with E=72.5 GPa, v=0.22. The epoxy matrix was

modeled by a nonlinear viscoelastic constitutive relation developed recently [13]. The reason for using a viscoelastic material description is that while the global strain rate during loading is constant, each matrix element in the RVE model would have different strains and strain rates. Hence, a rate-dependent model for the matrix would be more appropriate. A complete version of the viscoelastic constitutive model is provided in Ref. [13] and here, for the sake of completeness, only a brief description will be given.

For the uniaxial stress state, the model can be represented by a finite number of nonlinear Kelvin elements and a spring element, connected in series as shown in Fig.2.3. The constitutive equations generalized to the multiaxial stress state can be summarized as:

$$\{\dot{\varepsilon}_t\} = \{\dot{\varepsilon}_e\} + \{\dot{\varepsilon}_c\} \tag{2.10}$$

$$\{\dot{\varepsilon}_c\} = \sum_{i=1}^{n} \left(a_i [A] \sigma_{eq}^{\alpha_i - 1} \{\sigma\} - b_i \{\varepsilon_{ci}\} \right) \tag{2.11}$$

$$\{\dot{\sigma}\} = E[A]^{-1} \{\dot{\varepsilon}_e\} \tag{2.12}$$

in the above, $\{\dot{\varepsilon}_t\}$, $\{\dot{\varepsilon}_e\}$, $\{\dot{\varepsilon}_c\}$, $\{\dot{\sigma}\}$ are the total strain-rate, elastic strain-rate, creep strain-rate and stress-rate vectors (six components), respectively, and the matrix [A] is given by:

$$[A] = \begin{bmatrix} 1 & -\nu & -\nu & 0 & 0 & 0 \\ -\nu & 1 & -\nu & 0 & 0 & 0 \\ -\nu & -\nu & 1 & 0 & 0 & 0 \\ 0 & 0 & 0 & 1+\nu & 0 & 0 \\ 0 & 0 & 0 & 0 & 1+\nu & 0 \\ 0 & 0 & 0 & 0 & 0 & 1+\nu \end{bmatrix} \tag{2.13}$$

which is related to the value of Poisson's ratio. It is to be noted that instead of a linear relation between $\{\dot{\varepsilon}_c\}$ and $\{\sigma\}$, a power function relation is introduced through the

stress factor $\sigma_{eq}^{\alpha_i - 1}$ in equation (11), where $\sigma_{eq} = (\frac{3}{2} s_{ij} s_{ij})^{1/2}$ is the von Mises equivalent stress and $s_{ij} = \sigma_{ij} - \frac{1}{3}\delta_{ij}\sigma_{kk}$ is the deviatoric stress tensor.

Although theoretically any number of Kelvin elements can be chosen, it is unnecessary or too complicated to take more than two such elements. Based on test results, the material constants defined in equations (11) and (12) for the epoxy matrix were determined as follows:

$$a_1 = 5\times10^{-8}(\text{MPa})^{-2}, \quad \alpha_1 = 2, \; b_1 = 0.01,$$
$$a_2 = 1\times10^{-8}(\text{MPa})^{-2}, \quad \alpha_2 = 1, \; b_2 = 1\times10^{-6},$$
$$E = 2600\,\text{MPa} \text{ and } \nu = 0.4$$

Examples of the model predictions based on the above material constants and the comparison with the experimental results are shown in Figs.2.4 and 2.5. The effect of loading rates (constant stress rates) on the stress-strain response of the epoxy material is depicted in Fig.2.4. A stress relaxation test result can be seen in Fig.2.5. In this test the specimen was first loaded with a constant strain rate of 10^{-3} s^{-1} to reach a strain value of 0.74% (Fig.2.5a). Then the strain was held constant and it is seen that the stress gradually relaxes with the passing time (Fig.2.5b). This essentially confirms that the effect of residual stresses could be neglected in the present analysis.

The above viscoelastic material model has been implemented into the ADINA program through a user-supplied material model subroutine [17].

2.3 Damage Criterion for Epoxy Matrix and Implementation of Damage process in FEM Analysis

In general, damage mechanisms in laminate include four types of failure modes [18], i.e., matrix cracking, fiber-matrix interface debonding, delamination, and fiber rupture. Usually, matrix cracking (transverse cracking) is the first damage process to take place since the matrix has the lowest stress to failure of all the composite constituents [19-22]. Delaminations are often observed in the free edges. Delaminations are matrix cracks between plies that appear in certain type of laminates near the final failure stage. It is shown from the experiments of $[0_2,90_3]_S$ cross-ply laminates [23] that the transverse matrix cracking in the matrix of 90° plies could occur at an applied global strain of about 0.5-0.6%. In contrast, the onset of delamination in this cross-ply laminate was observed at an applied global strain greater than 2%. Therefore, for this laminate structure the dominant damage mode is the matrix transverse cracking. A matrix damage criterion must be introduced into the finite element analysis of the RVE model in order to simulate the damage initiation and evolution in the laminate.

Although the RVE model discussed here is subjected to a uniaxial loading, the stress in individual elements of the model is in a tri-axial stress state. Hence, a multiaxial damage criterion is required. Development of a proper multiaxial damage criterion for both polymer matrix and composite is a challenging topic. However, in this study, the maximum principal strain was used for predicting the matrix cracking, i.e., if $\varepsilon_1 \geq \varepsilon_f$, the matrix would crack, where ε_1 and ε_f are the maximum principal strain and failure strain of matrix, respectively. The failure strain of matrix is the threshold strain below which no damage would occur and is assumed to be a material constant. From

the experimental results on the epoxy specimens [13], it was found that in most tests the failure strains were less than 3%. Therefore, the failure strain in this study is taken to be equal to 0.03. In the finite element analysis, each matrix element is represented by the viscoelastic model, Eqs. (10)-(13) until the maximum principal strain of that matrix element is equal to, or exceeded the failure strain. It has been a common practice in simulating material damage by reducing the stiffness (or stiffness in a particular direction) to a near zero value. This is appropriate only for the analysis based on the deformation theories, in which the constitutive models are expressed in terms of the total stress and total strain vectors. For the current epoxy matrix, which is a time- and path-dependent material, an incremental relation between the stress and strain vectors must be adopted. If the stiffness reduction method is used after the principle strain exceeds the critical value, the stress will keep constant upon increase of the deformation. To simulate the matrix failure more accurately, the matrix element is governed by the following constitutive relation beyond the failure strain:

$$\{\dot{\sigma}\} = \beta E[A]^{-1}\{\dot{\varepsilon}\} - \alpha\{\sigma\} \tag{2.14}$$

where β is a small number ($=10^{-4}$) and α is a constant ($=0.01$). The above constitutive relation could reduce the stress vector to a very small value in a short duration of time ($\{\sigma\} = 0$ is the limit case), and thus, the matrix element would not carry further load. Figure 2.6 shows the response of the pure matrix material under a monotonic loading after the above failure criterion was introduced in the material model (only one matrix element was used). It could be seen that before reaching the failure strain, the element response is viscoelastic, whereas upon exceeding the failure strain, the stress drops

drastically to zero, thus simulating the damage process. For the sake of comparison, the response to the reduction in the stiffness only ($\beta=10^{-4}$, $\alpha=0$) is also provided in Fig.2.6 (dashed line).

2.4 Numerical Results and Comparison with Experiments

The model prediction for $[0,90_3,0]_T$ laminate under uniaxial loading with a constant strain rate of 10^{-5} s^{-1} is shown in Fig.2.7. It is seen that the numerical result is in good agreement with the experimental data. The finite element prediction without the introduction of damage mechanism is also shown in Fig.2.7. It is obvious that the later can only predict the initial linear response but is unable to predict the observed stiffness loss of the laminate caused by the matrix damage.

Figures 2.8 and 2.9 show the distributions of the stress and principal strain in the RVE when the global strain value is 0.58%. The σ_{xx} stress component values range from a tensile value of 426MPa to a compressive value of –8 MPa, while the principal strain varies *from 0.0294 to 0.000717*. The maximum value of σ_{xx} stress component occurs in the 0° fiber and the maximum value of σ_{xx} stress component in the epoxy matrix is about 75MPa. From Fig. 2.9, it is seen that the maximum principal strain appears in the matrix zone above the 90° fibers. The direction of the maximum principal strain in this zone is almost parallel to the loading direction (X-direction). The most important observation in these two figures is that while the applied global strain is about 0.6%, the maximum local principal strain in the epoxy matrix has almost reached 3%, i.e. the failure threshold value. Thus, any further increase in loading would cause the matrix to crack. Figure 2.10 shows the damage growth in the composite with the

increasing applied global strain. Because the strains in the matrix of 90° layers are almost uniformly distributed along the transverse direction (Fig.2.9, Z-direction), damage bands are first formed across the transverse direction when the global strain reaches a value of 0.6% (Fig.2.10a). Thereafter, the bands extend in Y-direction (Fig.2.10b), across the thickness of the laminate. At the global strain of 1.21%, the damage bands are connected in the 90° layers but are blocked by the 0° layer (Fig.2.10c). The above damage growth mode is in agreement with the experimental observation of the coupon specimens, where transverse cracks began to appear at a global strain value of about 0.6%. The cracks were formed immediately across the full width of the specimens. (Z-direction) Therefore, both experimental and numerical results confirmed that the dominant damage mechanism is the transverse matrix cracks in the 90° layers of the laminate.

In terms of prediction of the global stress-strain response for this cross-ply laminate, an elastic solution with a damage criterion or even the classical laminate theory with fully discounted plies at failure, may also be able to simulate the bilinear response. As an illustrative example, the results of a purely elastic matrix model incorporating the same damage criterion (i.e. the material constants a_1, a_2, b_1 and b_2 in equation (11) are set to zero.) are presented. It can be seen from Fig.2.7 that with respect to the overall response, the prediction of the elastic solution is not much different from that of the viscoelastic matrix model. However, there are some differences concerning with the predicted damage initiation and propagation, see Fig. 2.11. The elastic solution predicts a delayed initiation of the transverse cracking (at a global strain of 0.64%, i.e. increase of over 10%). Moreover, in the elastic solution the

propagation of the transverse crack is slower, and it does not propagate across the full thickness of the 90° layers until the global strain level reaches a value of 1.68% versus 1.21% for the viscoelastic matrix. Therefore, the viscoelastic solution appears to provide a more accurate prediction of damage initiation and propagation than the elastic solution.

2.5 Conclusions

A meso/micro-mechanical analysis of a $[0,90_3,0]_T$ laminate has been reported. The approach was based on a finite element analysis of a multi-layer unit cell model. The model prediction was in good agreement with the experiment observation not only in global stress-strain response but also in the initiation and propagation of the transverse matrix damage. The success of the analysis can be attributed to the following key points in the current meso/micro-mechanical model:

1. The multi-layer unit cell model provides a more accurate representation of the laminate lay-up structure.
2. The nonlinear viscoelastic constitutive model describes more accurately the multi-axial stress-strain relation of the epoxy matrix material.
3. The damage criterion introduced for the epoxy matrix enables one to simulate the damage initiation and growth observed in the experimental investigations.

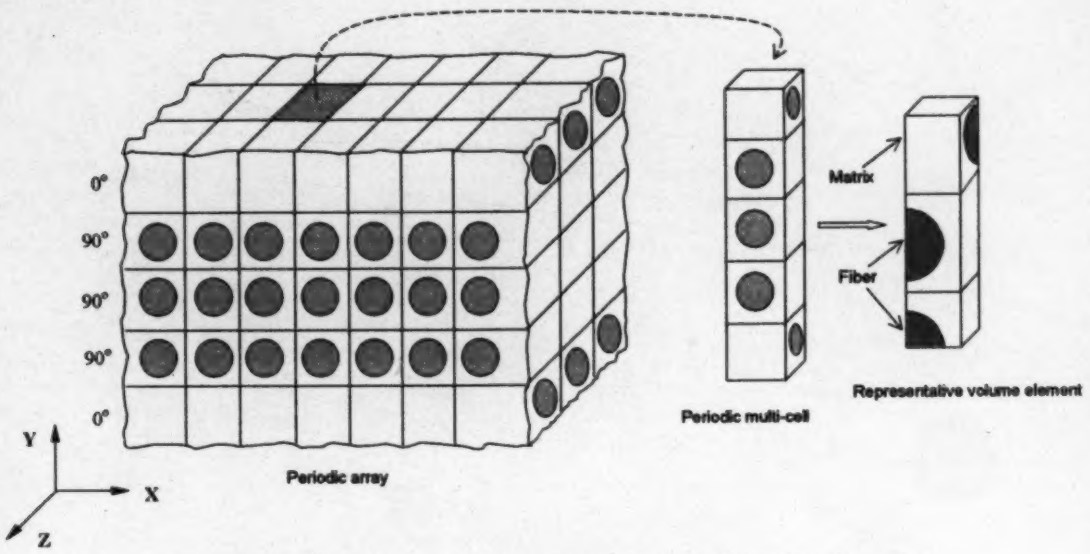

Figure 2.1 Representative Volume Element for $[0/90_3/0]_T$ laminate

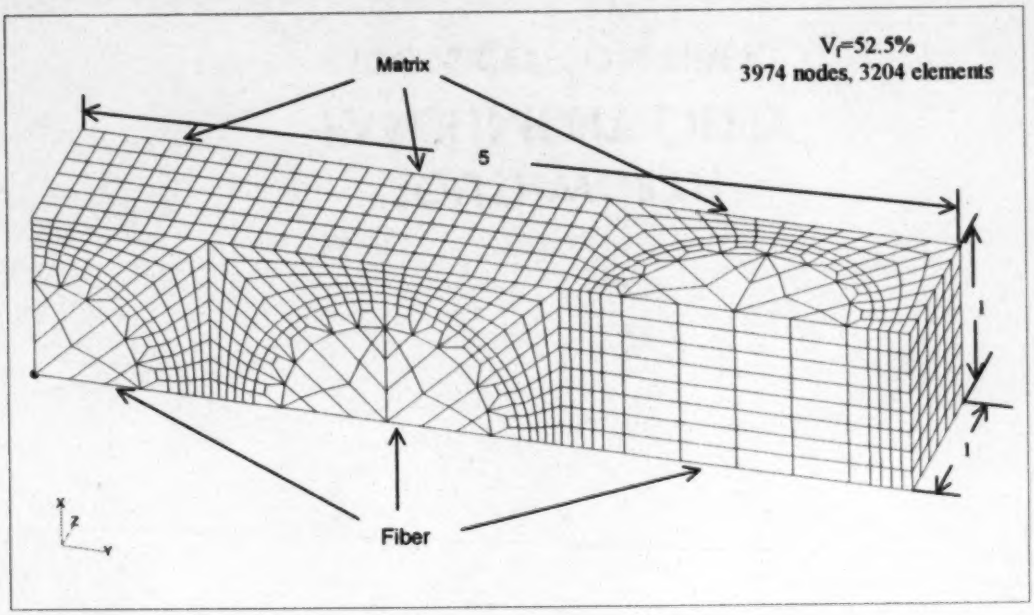

Figure 2.2 Three-dimensional finite element mesh for RVE of $[0/90_3/0]_T$ laminate

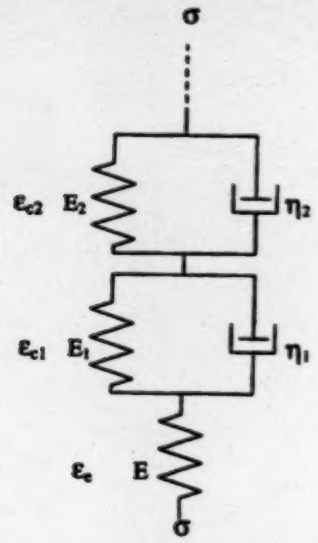

Figure 2.3. A viscoelastic model represented by a finite series of Kelvin elements coupled with an elastic spring

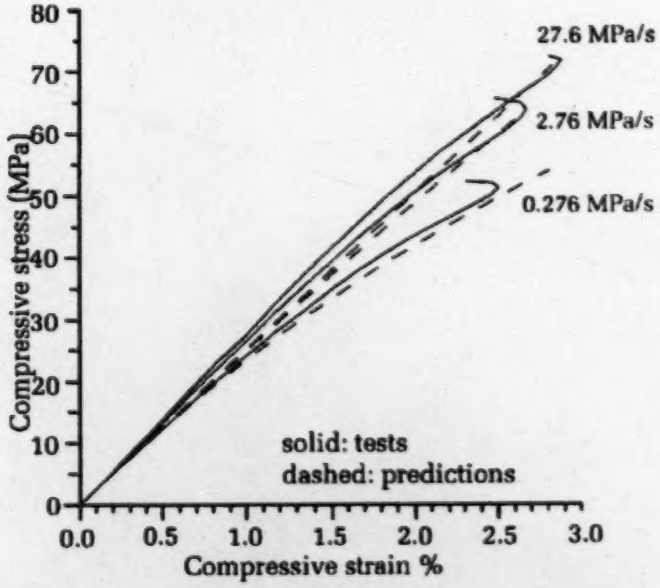

Figure 2.4 Stress-strain curves of epoxy under uniaxial tests with different stress rates

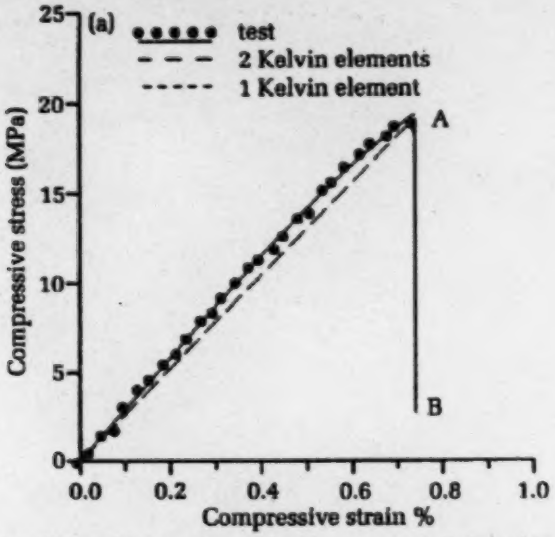

a) loading with a constant strain rate to A & keeping strain constant

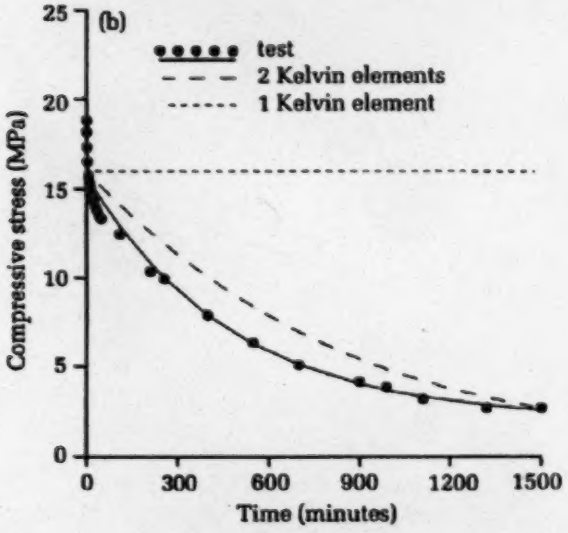

b) stress relaxation with the passing time

Figure 2.5 A stress relaxation test result and model prediction for epoxy matrix

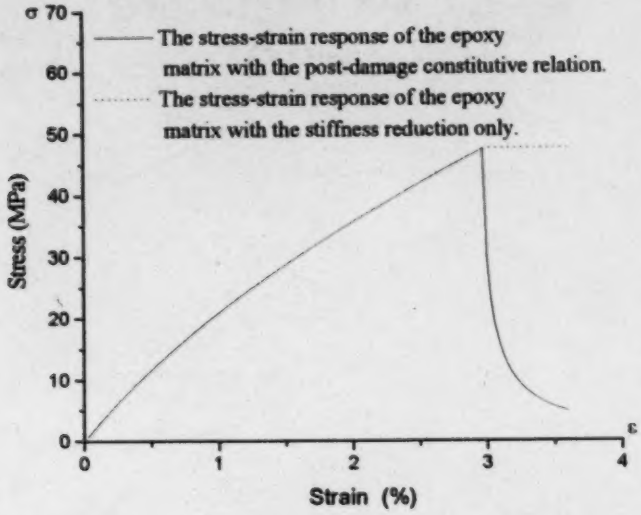

Figure 2.6 Stress-strain curve of epoxy with damage criterion

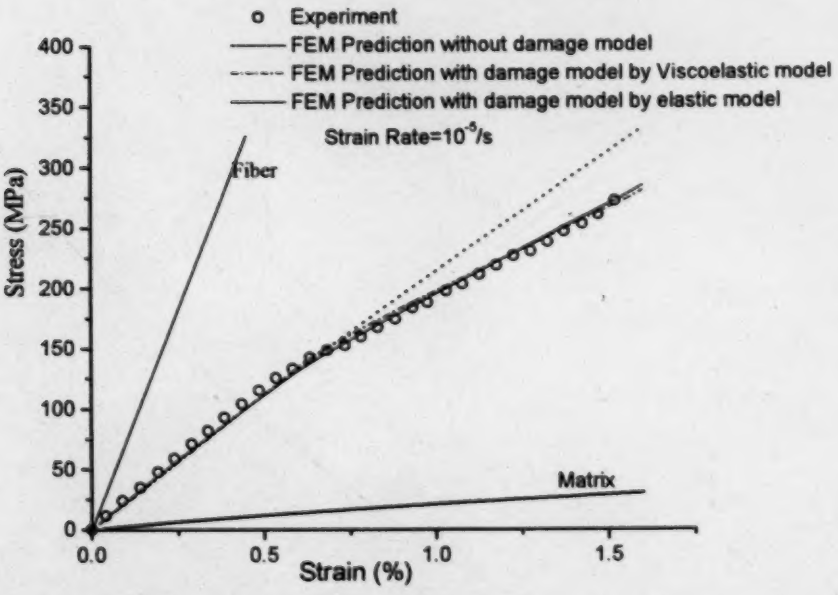

Figure 2.7 FEM Predicted stress-strain curves of $[0/90_3/0]_T$ laminate with and without damage analysis

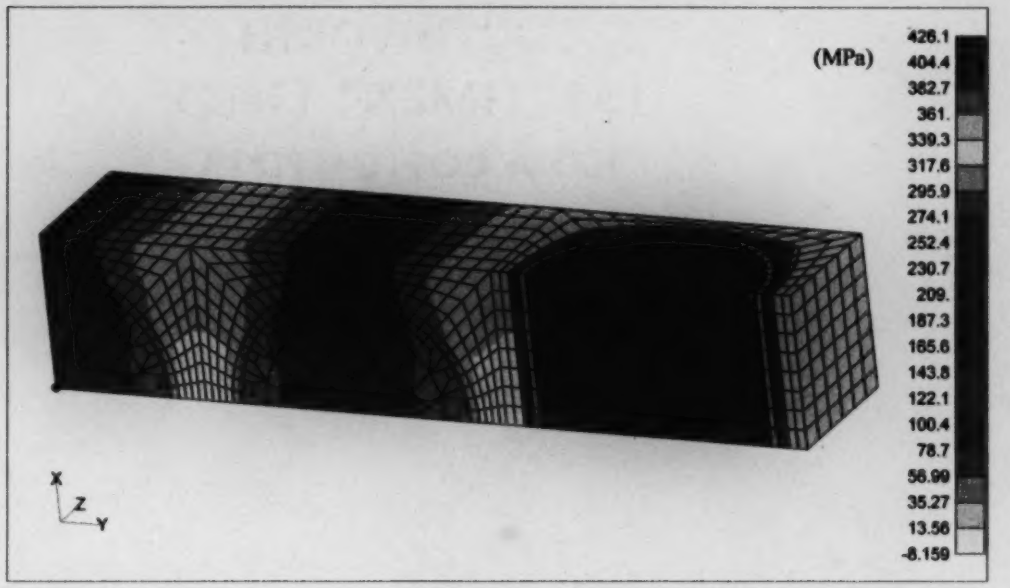

Figure 2.8 Stress distribution of σ_{xx} component at the applied global strain value of 0.58%

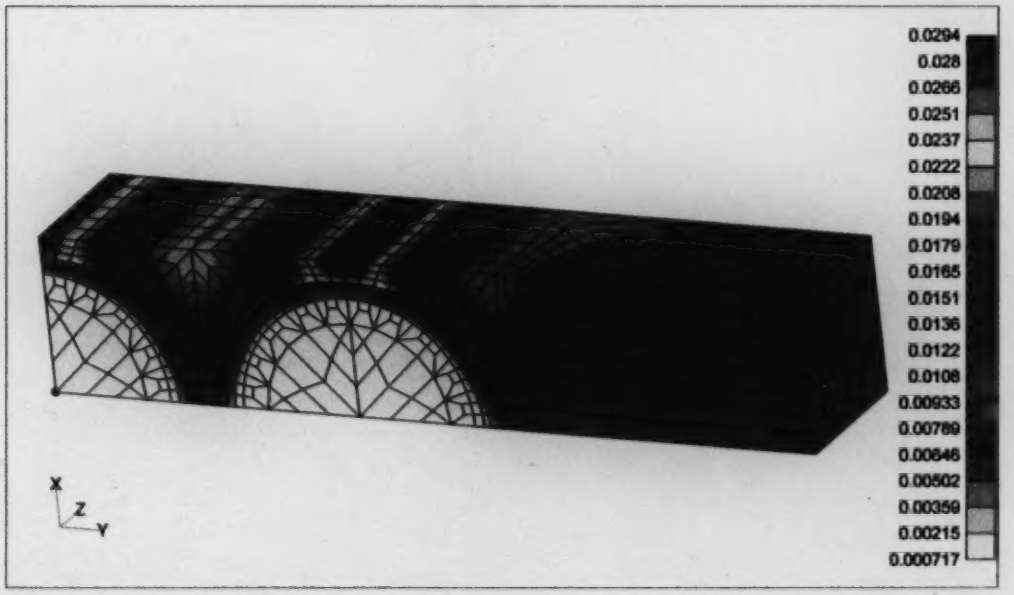

Figure 2.9 Maximum principal strain distribution at the applied global strain value of 0.58%

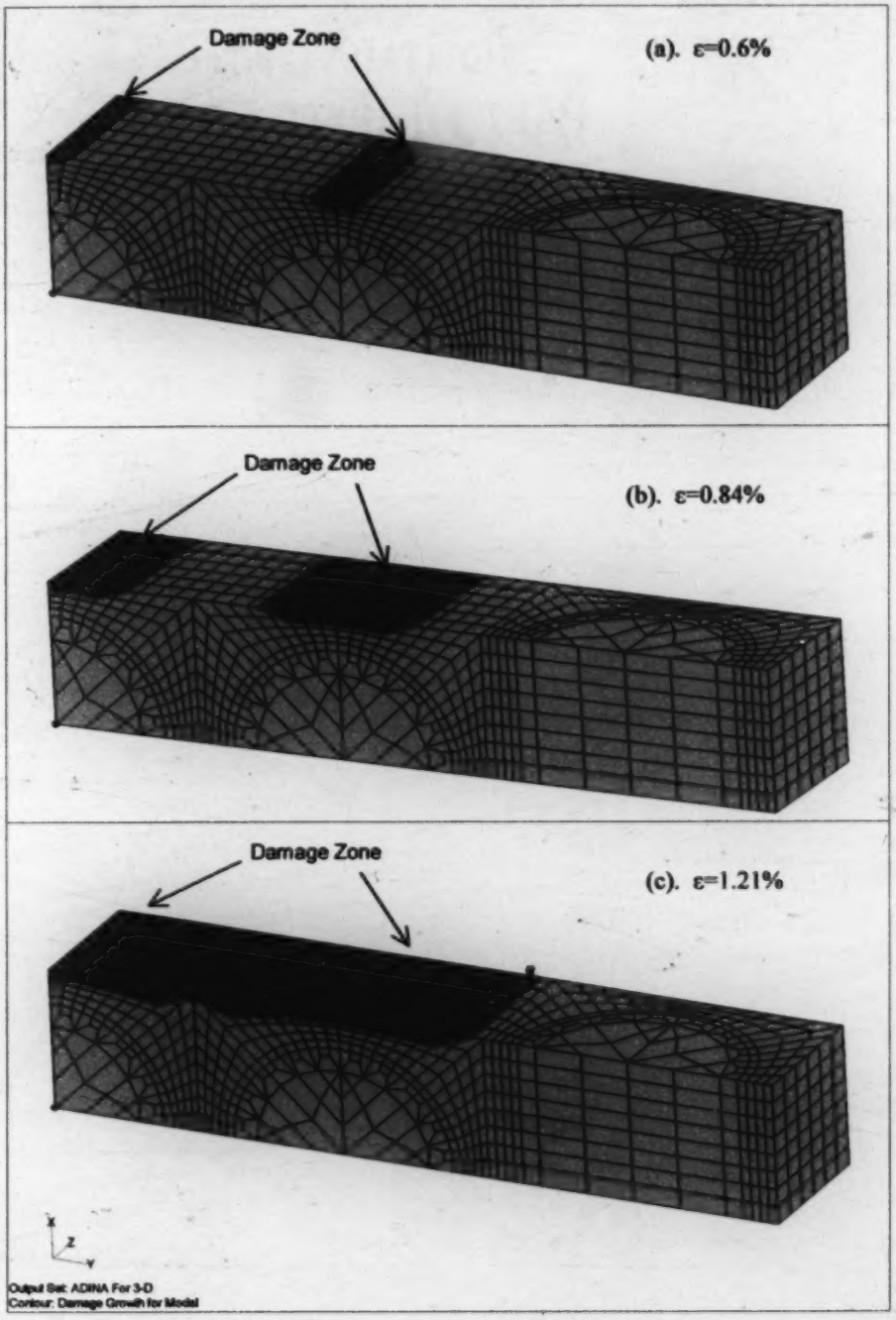

Figure 2.10 Damage Growth in the RVE model

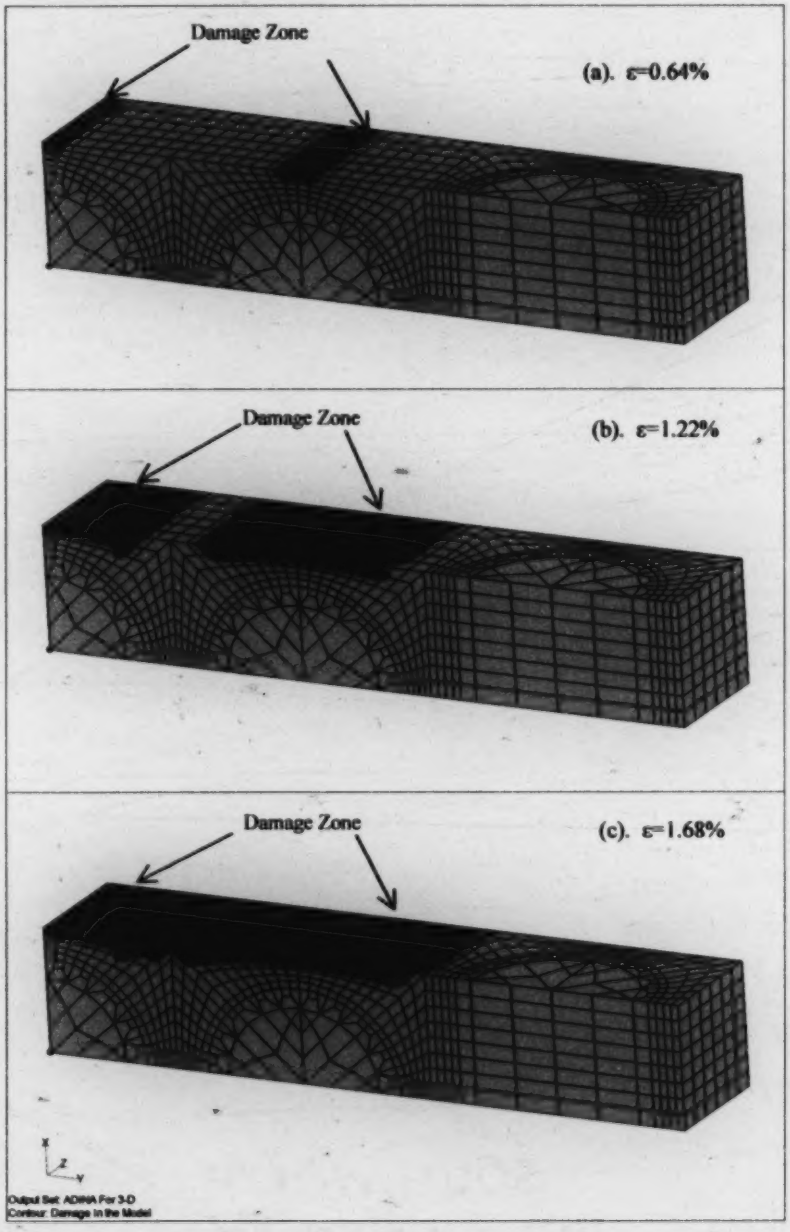

Figure 2.11 Damage growth in the RVE model by elastic solution with damage criterion

Bibliography

1. Sun, C.T. and Chen, J.L., "A simple flow rule for characterizing nonlinear behavior of fiber composites," *Journal of Composite Material*, Vol. 23, 1989, pp1009-1020.
2. Aboudi, J., "Micromechanical analysis of composites by the method of cells," *Applied Mechanics Review*, Vol.42, 1989, pp193-221.
3. Nemat-Nasser, S. and Hori, M., "Micromechanics: Overall Properties of Heterogeneous Materials, " Elsevier Science Publishers, Admsterdam, 1993.
4. Kim, S.J., and Shim, E.S., "A thermoviscoplastic theory for composite materials by using a matrix-partitioned unmixing-mixing scheme," *Journal of Composite Materials*, Vol.30, 1996, pp1647-1699.
5. Lissenden, C.J. and Herakovich, C.T., "Numerical Modeling of Damage Development and Viscoplasticity in Metal Matrix Composites," *Computer Method in Applied Mechanics and Engineering*, Vol.126, 1995, pp289-303.
6. Annth, C.R., Mukherjee, S. and Chandra, N., "Effect of Time-dependent Matrix Behavior on the Evolution of Processing-induced Residual Stress in Metal Matrix Composites," *Journal of Composite Technology & Research*, Vol.19, 1997, pp134-141.
7. Adams, D.F. and Crane, D.A., "Finite element micromechanical analysis of a unidirectional composite including longitudinal shear loading," *Computer and Structures*, Vol.18, 1984, pp-1153-1165.
8. Aboudi, J., "Micromechanical prediction of initial and subsequent yield surfaces of metal matrix composites," *International Journal of Plasticity*, Vol.6, 1990, pp471-484.
9. Allen, D.H. and Boyd, J.G., "Convergence rates for computational predictions of stiffness loss in metal matrix composites," *Composite Materials and Structures*, AMD-Vol. 179/AD-Vol.37, 1993, pp31-45.
10. Bonora, N., Costanzi, M., Newaz, G., and Marchetti, M., "Micro-damage effect on the overall response of long fiber/metal matrix composites," *Composites*, Vol.25, 1994, pp575-582.

11. Pindera, M-J., and Aboudi, J., "Micromechanical Analysis of Yielding of Metal Matrix Composites," *International Journal of Plasticity*, Vol. 4, 1988, pp195-214.

12. Bigelow, C.A., "Thermal Residual Stresses in a Silicon-Carbide/Titanium [0/90] laminate", *Journal of Composites Technology and Research*, Vol.15, 1993, pp304-310.

13. Xia, Z. and Ellyin, F., "Time-dependent behavior and viscoelastic constitutive modeling of an epoxy polymer", *Polymers & Polymer Composites*, Vol.6, 1998, pp75-83.

14. Hoover, J.W., Kujawski, D. and Ellyin, F. "Transverse cracking in symmetric and unsymmetric glass fiber/epoxy matrix laminates," *Composite Science and Technology*, Vol.57, 1997, pp1513-1526.

15. Roberston, D.D. and Mall, S., "Micromechanical relations for fiber-reinforced composite using the free transverse shear approach," *Journal of Composite Technology & Research*, Vol.15, 1993, pp181-192.

16. Sun, C.T., and Vaidya, R.S., "Prediction of composite properties from a representative volume element," *Composite Science and Technology*, Vol.56 1996, pp171-179.

17. ADINA, User Manual 1984, ADINA Engineering Inc. Watertown, MA.

18. Harris, C.E., Coats, T.W., Allen, D.H., and Lo,D.C., " A Progressive Damage Model and Analysis Methodology for Predicting the Residual Strength of Composite Laminates," *Journal of Composite Technology & Research*, Vol. 19, 1997, pp3-9.

19. Laws, N., " Progressive Transverse Cracking in Composite Laminates," *Journal of Composite Materials*, Vol. 22, 1988, pp900-915.

20. Daniel, I. M., and Lee J.W.," Damage Development in Composite Laminates under Monotonic Loading," *J. of Composite Technology & Research*, Vol.12, 1990, pp98-102.

21. Jen, K.C., and Sun, C.T.," Matrix Cracking and Delamination Prediction in Graphite/Epoxy Laminates," *Journal of Reinforced Plastics and Composites*, Vol.11, 1992, pp1163-1175.

22. Salpekar, S.A., "Analysis of Delamination in Cross-ply Laminates initiating from Impact induced Matrix Cracking," *Journal of Composite Technology & Research*, Vol.15, 1993, pp. 88-94.

23. Hoover, J.W., "Transverse Cracking of $[\pm\theta,90_3]_s$ Composite Laminates", M.Sc. Thesis, Department of Mechanical Engineering, University of Alberta, 1999.

Chapter 3

Finite Element Mircromechanical Modeling of Free Edge Effects in Glass Fiber/Epoxy Cross-ply Laminates

3.1 Introduction

The increasing usage of continuous fiber-reinforced polymeric composites in load bearing applications requires the methods to predict the mechanical properties and damage mechanisms of these materials accurately, in order to design more damage tolerant structures. Consequently, the objective of designing composite structures with optimized damage characteristics has led to the development of mechanical theories for the modeling of composite at macromechanical and micromechanical levels. Classical laminate theory (CLT) is a widely accepted macromechanical method for many aspects of the mechanical behavior of composite laminates. In classical laminate theory, the material properties of each ply are averaged or smeared to produce a global orthotropic material, which is used to calculate the stresses and strains in each ply [1]. One of its limitations, however, is the description of damage initiation and propagation in the laminates. The often adopted first ply failure criterion [1] can approximately predict the transverse matrix cracking based on the averaged or smeared composite stresses and strains, but can not predict the crack initiation site and propagation path in the laminates [2]. In particular, the CLT has difficulties in predicting the free edge effects in laminated composites because damage may occur early in the life of the composites due

to the free edge effects but may have only a small effect on the overall stiffness and strength properties.

Therefore, to predict the damage initiation and propagation in composites accurately, the fibrous composites must be modeled at the fiber and matrix levels [3]. The use of finite element micromechanics provides a powerful tool to investigate the stress/strain state of composites on the microscale in terms of their constituent material properties. The micromechanical modeling has the advantage of providing more physical information of the constituent fiber and matrix so as to numerically simulate the failure of fiber and matrix as well as interface debonding between the two. Considerable research efforts have been undertaken to investigate damage and failure of unidirectional fiber-reinforced composite by using finite element micromechanical modeling [4-8], but only few researchers [9] have extended this methodology to study the free edge effects. It is the goal of this study to investigate the role of free edge surface on the damage initiation and progression in the cross-ply laminates by a micromechanical modeling.

The aim of the present contribution is to determine the micromechanical stress/strain field at the free edge surface in $[0/90]_{ns}$ glass fiber/epoxy cross-ply laminate subjected to a uniaxial loading. A three-dimensional micromechanical model including the free edge surface of the cross ply laminate has been developed to carry out a finite element analysis. The analysis incorporates a nonlinear viscoelastic constitutive relation [10] particularly suited for the epoxy matrix. In order to simulate the damage progression in the cross-ply laminate, the maximum principle strain and the maximum normal traction are used as the failure criteria for the matrix element and interface

element, respectively. These criteria have been incorporated into the finite element analysis program, so as to predict the damage initiation as well as damage propagation near the free edge surface in the cross-ply laminates. For the comparative purpose, the damage evolution of the interior region of the composite, which is not influenced by the edge effects, is studied through a representative volume element (RVE). In addition, the predicted globe stress-strain response obtained by the RVE is also compared to the experimental results.

3.2 Micromechanical Modeling Approach

In the micromechanical model, it is assumed that fibers are uniformly dispersed within the homogeneous matrix, and packed in a square array. Figure 3.1 shows a representation of a thick cross-ply $[0/90]_{ns}$ laminate from the micromechanical point of view. The following assumptions dealing with this model are made in this type of representation:

a. The model is fully periodic in all three directions.

b. Fibers are circular and evenly spaced in the cross-ply laminate.

c. Each unidirectional layer could be represented by one row of fibers imbedded within the matrix.

d. The cell model has a constant fiber volume fraction of 52.5% as the full cross-ply laminate.

e. The model surfaces remain plane after deformation.

These assumptions allow for the analysis of the cross-ply $[0/90]_{ns}$ laminate to be performed on one identical representative volume element (RVE) as shown in Fig.3.1.

3.2.1 Finite Element Modeling of Free Edge Surface

The free edge effect of composite laminates has been investigated for sometime. A common numerical approach to this problem has been to model the entire laminate geometry using a three-dimensional finite element analysis [11-14], among others. This macromechanical approach treats each layer of composite laminates as a homogenous, orthotropic continuum and models the whole structure of laminates by layered finite elements. Although the fully three dimensional model has the advantage of representing the laminate at all locations, however there are limitations to this method related to computational restrictions imposed by a computer memory. Thus, in this type of model, only a few elements are placed along the free edge surface of the laminate, and this may results in an inaccurate representation of the stress and strain fields at the free edge surface. In addition, it is not possible to identify the stress/strain states in and between the fiber and matrix.

In order to alleviate the difficulties encountered by the macromechanical model, the representation of a cross-ply laminate based on the micromechanical modeling (see Fig.3.1) was selected to analyze the cross-ply laminate. Due to the periodic characteristic of this representation, a representative micromechanical element could be cut near the free surface as shown in Fig.3.2. This micromechanical model could be replicated in X-Y plane (Fig.3.2) to construct the entire free edge surface.

Numerical tests on this micromechanical model have shown that the free edge effect is localized near the free surface with a maximum length less than half of the fiber diameter (see in Fig.3.6). Consequently, all surfaces in Fig.3.2 follow the assumptions stated earlier, i.e. plane surfaces remain plane, except the free edge surface which could distort. Due to the symmetry and loading conditions, only 1/4 of this micromechanical model needs to be analyzed by the finite element method.

The model was meshed using three-dimensional, eight-node hexahedral elements. Figure 3.3 shows the finite element mesh and dimensions for the cross-ply [0/90] model near the free edge surface. This mesh density was determined in a previous study [15] to be suitable for the use in a three-dimensional cross-ply laminate analysis. Note that a very thin layer of interface element is introduced around each fiber for the treatment of interface debonding, which have the same material properties as the matrix. Moreover, the same micromechanical model that is not influenced by the edge effects, i.e. a fully periodic structure with no free edge surface (an interior RVE, Fig.3.1), has also been investigated for the sake of comparison. The only difference between these two models is the different boundary conditions applied on the free surface. In the analysis to follow, the micromechanical model with the free edge surface is called free edge model, whereas the one without the free edge surface is called interior model.

3.2.2 Applied Boundary Conditions

Symmetric conditions were applied to the two boundary surfaces X=0 and Y=0 of the finite element model in Fig.3.3, i.e.:

$$u(0, Y, Z) = 0 \tag{3.1}$$

$$v(X,0,Z) = 0 \tag{3.2}$$

In general, the free edge surface may not remain plane and it could have a slope discontinuity or distortion during the loading. For this case, the free surface (Z=2) in Fig.3.3 was modeled as a traction free surface (that is, no constraints were imposed). Hence, periodic boundary conditions were only applied on the surfaces X=1, Y=2 and Z=0 of the finite element model shown in Fig.3.3, i.e.

$$u(1,Y,Z) = u(1,0,0) \tag{3.3}$$

$$v(X,2,Z) = v(0,2,0) \tag{3.4}$$

$$w(X,Y,0) = w(1,2,0) \tag{3.5}$$

However, for the interior model, the surface (Z=2) is not a free surface, hence the periodic boundary conditions were applied on this surface, i.e.

$$w(X,Y,2) = w(0,0,2) \tag{3.6}$$

The applied uniaxial mechanical loading was simulated by applying the prescribed displacements on X=1 surface in X direction. The effect of residual thermal stresses on the cross-ply laminate has also been studied in a previous study [15]. It has been shown that the effect of residual stresses could be neglected for the *viscoelastic* composites.

3.3 Materials Model for the Fiber and Epoxy Matrix

In this study, the glass fiber is assumed to remain linear elastic, and is thus modeled by the generalized Hooke's law, with E=72.5 GPa, and v=0.22. The epoxy matrix is modeled by a nonlinear viscoelastic constitutive relation recently developed

by Xia and Ellyin [10]. A complete version of the viscoelastic constitutive model is provided in Ref. [10] and here, for the sake of completeness, only a brief description will be given.

For the *uniaxial* stress state, the model can be represented by a finite number of nonlinear Kelvin elements and a spring element, connected in series as shown in Fig.3.4. The constitutive equations, generalized to the multiaxial stress state, are summarized below:

$$\{\dot{\varepsilon}_t\} = \{\dot{\varepsilon}_e\} + \{\dot{\varepsilon}_c\} \tag{3.7}$$

$$\{\dot{\varepsilon}_c\} = \sum_{i=1}^{n} \left(a_i [A] \sigma_{eq}^{\alpha_i - 1} \{\sigma\} - b_i \{\varepsilon_{ci}\} \right) \tag{3.8}$$

$$\{\dot{\sigma}\} = E[A]^{-1} \{\dot{\varepsilon}_e\} \tag{3.9}$$

In the above, $\{\dot{\varepsilon}_t\}$, $\{\dot{\varepsilon}_e\}$, $\{\dot{\varepsilon}_c\}$, $\{\dot{\sigma}\}$ are the total strain-rate, elastic strain-rate, creep strain-rate and stress-rate vectors (six components), respectively. The matrix [A] is given by:

$$[A] = \begin{bmatrix} 1 & -\nu & -\nu & 0 & 0 & 0 \\ -\nu & 1 & -\nu & 0 & 0 & 0 \\ -\nu & -\nu & 1 & 0 & 0 & 0 \\ 0 & 0 & 0 & 1+\nu & 0 & 0 \\ 0 & 0 & 0 & 0 & 1+\nu & 0 \\ 0 & 0 & 0 & 0 & 0 & 1+\nu \end{bmatrix} \tag{3.10}$$

which is related to the value of Poisson's ratio. It is to be noted that instead of a linear relation between $\{\dot{\varepsilon}_c\}$ and $\{\sigma\}$, a power function relation is introduced through the stress factor $\sigma_{eq}^{\alpha_i - 1}$ in equation (8), where $\sigma_{eq} = (\frac{3}{2} s_{ij} s_{ij})^{1/2}$ is the von Mises equivalent stress and $s_{ij} = \sigma_{ij} - \frac{1}{3}\delta_{ij}\sigma_{kk}$ is the deviatoric stress tensor.

Although any number of Kelvin elements can be chosen, it is shown in Ref. [10] that two elements are sufficient. Based on test results, the material constants defined in equations (8) and (9) for the epoxy matrix were determined as follows:

$$a_1 = 5\times10^{-4}(\text{MPa})^{-2}, \quad \alpha_1 = 2,\ b_1 = 0.01,$$
$$a_2 = 1\times10^{-4}(\text{MPa})^{-2}, \quad \alpha_2 = 1,\ b_2 = 1\times10^{-6},$$
$$E = 2600\,\text{MPa},\ \nu = 0.4$$

The above viscoelastic material model has been implemented into the ADINA finite element program through a user-supplied material model subroutine [16].

3.4 Modeling Damage Initiation and Propagation in Finite Element Analysis

Typical damage mechanisms in the micromechanical analysis of composites include matrix cracking, fiber-matrix interface debonding, and fiber fracture [4]. Matrix cracking is a common damage type in a fibrous composite. It is found experimentally [17-19] that the transverse matrix cracking in the cross-ply laminates may occur in the early stage of loading, a fraction of the ultimate strain of composite. Consequently, matrix cracking (transverse cracking) is usually considered to be the first damage process taking place in the cross-ply laminate. A damage criterion needs to be incorporated into the finite element micromechanical model in order to simulate the damage initiation and its evolution in the laminate. In addition, it is shown in Ref. [20] that the free edge surface of a laminate is a favored site for the interfacial debonding because of the presence of high tensile stresses in this area. Therefore, another damage criterion must be specified to simulate the interface-debonding process.

Hence, the damage mechanisms used in the finite element micromechanical model studied herein are the matrix cracking and interface debonding. The maximum principal strain was used as the damage criterion for matrix cracking, i.e., when $\varepsilon_1 \geq \varepsilon_f$, the matrix would crack, where ε_1 and ε_f are the maximum principal strain and failure strain of matrix, respectively. The failure strain of the matrix is the threshold strain below which no damage would occur and is assumed to be a material constant. From the experimental results on the epoxy specimens [10], it was found that in most tests the failure strains were less than 3%. Therefore, the failure strain in this study is taken to be equal to 0.03. In the finite element analysis, for a given macroscopic stress/strain state, the damage criterion was checked for each matrix element in the micromechanical model. Each matrix element is initially represented by the viscoelastic model, Eqs. (7)-(9), until the maximum principal strain in the matrix element becomes equal to, or exceeded the failure strain. Beyond this failure strain, the matrix element property is governed by the following constitutive relation:

$$\{\dot{\sigma}\} = \beta E[A]^{-1}\{\dot{\varepsilon}\} - \alpha\{\sigma\} \tag{3.11}$$

where β is a small number ($=10^{-4}$) and α is a constant ($=0.01$). The above constitutive relation reduces the stress vector to a very small value in a short duration of time ($\{\sigma\} = 0$ is the limit case), and thus, the matrix element could not carry any further load. Figure 3.5 shows the response of the pure matrix material under a monotonic loading, and the post failure response with the above relation introduced in the material model (only one matrix element was used). It could be seen that before reaching the failure

strain, the element response is viscoelastic, whereas upon exceeding the failure strain, the stress drops drastically to zero, thus simulating the damage process.

It was mentioned earlier that a very thin layer of interface elements, with the same material property as the matrix, was introduced around each fiber in the micromechanical model. This group of elements is used to simulate an interface debonding. The maximum radial stress (normal to the interface) is used as the damage criterion for the interfacial debonding, i.e. once the normal traction (tensile) in an interface element reaches the interface failure stress, $T_n > T_c$, then that element is assumed to undergo damage and can not carry any load. The damage simulation process for the interface debonding in the finite element analysis is the same as that of the matrix cracking, except that a different damage initiation criterion is used for interface element (critical normal stress criterion). There is a lack of the experimental data regarding to the value of critical stress, T_c, hence based on the available information the normal traction (tensile) strength of the interface, was taken to be 101 MPa.

The above criteria for the initiation of damage along with the post-damage constitutive relation have been implemented into the ADINA finite element program through the user-supplied material model subroutine [16]. Thus, with the incrementally applied global stress/strain, the damage initiation site and its evolution could be obtained from the above described micromechanical model.

3.5 Results and Discussion

Figure 3.6 shows the distribution of the maximum principle strain near the free edge surface obtained from the free edge model when the applied uniaxial strain has reached 0.52%. For the sake of comparison, the distribution of the maximum principle strain obtained from the interior model at the same overall strain level is also shown in the same figure (note that the local strain values for the same color are different for each model). It is seen that the maximum value of the principle strain on the interior model takes place in the matrix zone on the top of 90° fiber, whereas the maximum value on the free edge model occurs in the matrix zone near the interface. While the maximum value of principle strain on the interior surface is 2.55%, that value on the free edge surface is 2.91%, almost equal to the failure strain of the matrix. Thus, for a given far field strain state, the maximum principle strain occurs on the free edge surface of the cross-ply laminate. In addition, it can been seen that the free edge effect is localized near the free edge surface. The strain distribution half fiber diameter away from the free edge surface is almost the same as the strain distribution of the interior RVE model.

The advantage of the current micromechanical model is that it could give a detailed stress/strain distribution in and between the fiber and matrix in a micro-level scale. It provides physical information for the determination of the damage initiation in the laminate. With the proper damage criterion and simulation of damage propagation, the damage evolution in the laminate could be predicted from the model. Figures 3.7 and 3.8 depict the damage initiation and growth in the laminate with the increasing value of the global strain. It is found that, at a global strain of 0.52%, a crack begins to

form in the matrix zone near the interface on the free edge surface. This damage, however, is confined to the interface region on the free edge surface. No damage is initiated on the other surface (interior surface) of this model. With the increased global strain to 0.56%, more damage is initiated on the top of 90° fiber, but it is still localized near the free edge surface. When the global strain reaches about 0.6%, the matrix crack on the top of 90° fiber propagates in the transverse directions (Fig.3.7c, Z-direction), whereas the interfacial damage is confined to the free edge surface, and has propagated around the interface on the free surface but has not evolved in the transverse direction.

Thereafter, the transverse matrix cracking extend in the Y-direction (Fig.3.8b), across the thickness of the laminate, in the meantime, the crack near the interface begins to propagate in the transverse direction (Fig.3.8b, Z-direction). It should be noted from Fig.3.8 that the cracks in the matrix or the interface always tend to propagate near the free edge surface first, then expand into the interior.

In order to demonstrate the unique feature of the damage growth near the free edge surface, the prediction of damage obtained from the interior model is shown in Fig.3.9. In this case, the damage initiation occurs at a global strain of about 0.64%, much higher than that of free edge model (see Fig.3.7a and Fig.3.9a). In addition, once the crack has formed, it propagates in the transverse direction (Fig.3.9, Z-direction) immediately. Furthermore, the interfacial crack initiates after transverse matrix cracking.

The above damage growth model for the free edge surface is also in agreement with the experimental observation [21-22]. References [21] and [22] also confirmed that the crack tends to grow initially along the free edge, propagate into the interior of the

laminate. Thus, the micromechanical model near the free edge provides reliable prediction of the damage growth in the laminate when compared with the experimental results.

It was mentioned earlier that the free edge effects are localized near the free surface. In terms of predicting the global stress-stain response of this cross-ply laminate, this narrow zone will have little effect on the overall properties of the laminates. The prediction of interior model including the damage analysis, which is not influenced by the edge effects, is compared with our experimental results for this cross-ply laminate in Fig.3.10. For a comparative purpose, the same RVE model without damage analysis is also shown in Fig.3.10. It is obvious that the RVE model without the edge effects but with the damage analysis can predict the linear and nonlinear parts quite accurately; while the same model, but without the edge effects and the damage analysis, can only predict the initial linear response, and is incapable of predicting the observed stiffness loss of the laminate. This figure shows that the damage analysis is the most important feature when attempting to predict the global stress-strain response of the cross-ply laminates. The free edge effects, however, have insignificant effect on the global stress-strain response of the cross-ply laminate despite their significant influence on the damage initiation and propagation in the cross-ply laminate.

3.6 Conclusions

A micromechanical model and two damage criteria were incorporated into the finite element analysis to study the free edge effects on the damage initiation and propagation in cross-ply laminates. The micromechanical model provides useful micro-

level stress/strain state near the free edge surface. This stress/strain state was used in conjunction with the damage criteria to investigate damage progress in the cross-ply laminate. The implementation of the damage process in the present numerical study was computationally efficient in investigating the free edge effects. This method provided reliable predictions of the damage process in the cross-ply laminates. The following conclusions are drawn from the present study:

1. The magnitude of stress/strain state near the free edge surface is higher that one in the interior surface.
2. Due to the free edge effects, damage initiates at the free surface, and propagates into the interior of the cross-ply laminate. The crack initiates at lower a global strain on free edge surface compared with that at the interior model.
3. Although damage initiation occurs early near the interface on the free edge surface, the transverse matrix cracking which initiates later on, propagates first into the interior of the cross-ply laminate.
4. The early damage initiation on the free edge surface, however, has negligible effect on the global mechanical properties of the cross-ply laminate.

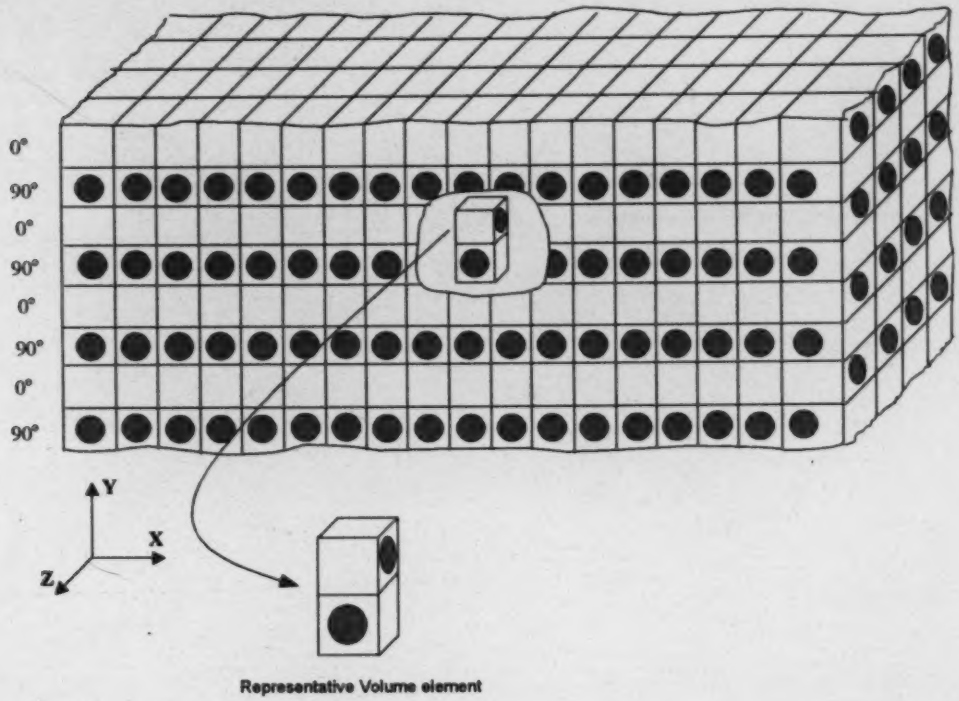

Figure 3.1. Micromechanical Representation of an interior element of $[0/90]_{ns}$ cross-ply laminate.

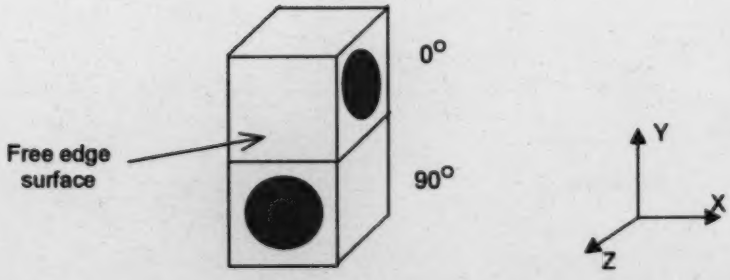

Figure 3.2. A representative micromechanical model near free edge surface for $[0/90]_{ns}$ laminate

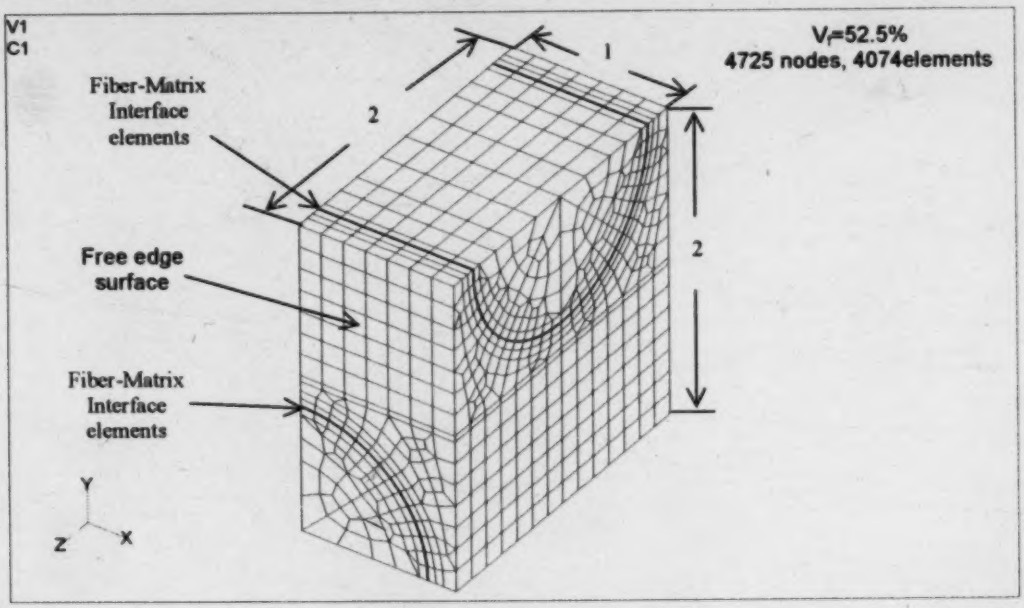

Figure 3.3 Three-dimensional finite element mesh of micromechanical model near free edge surface for $[0/90]_{ns}$ laminate

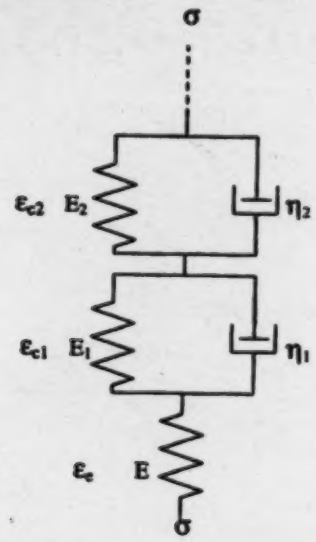

Figure 3.4. A viscoelastic model represented by a finite series of Kelvin elements coupled with an elastic spring

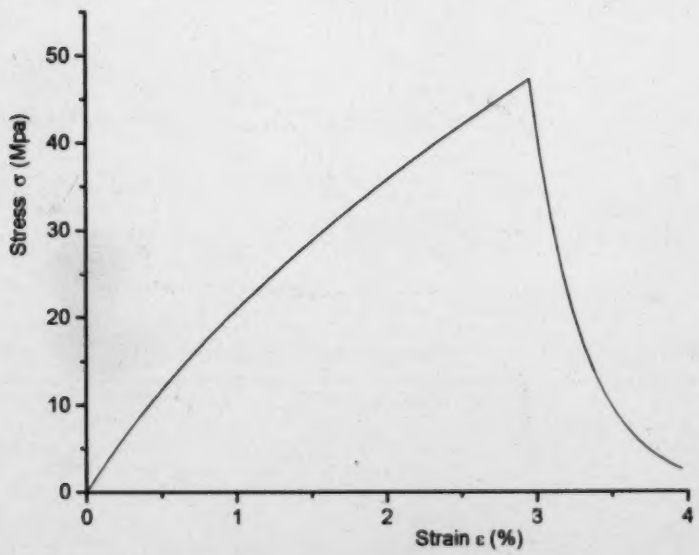

Figure 3.5 Stress-strain response of an epoxy matrix element with the damage criterion of the maximum principle strain.

Figure 3.6 Maximum principal strain distribution at the applied global strain value of 0.52% by two different models

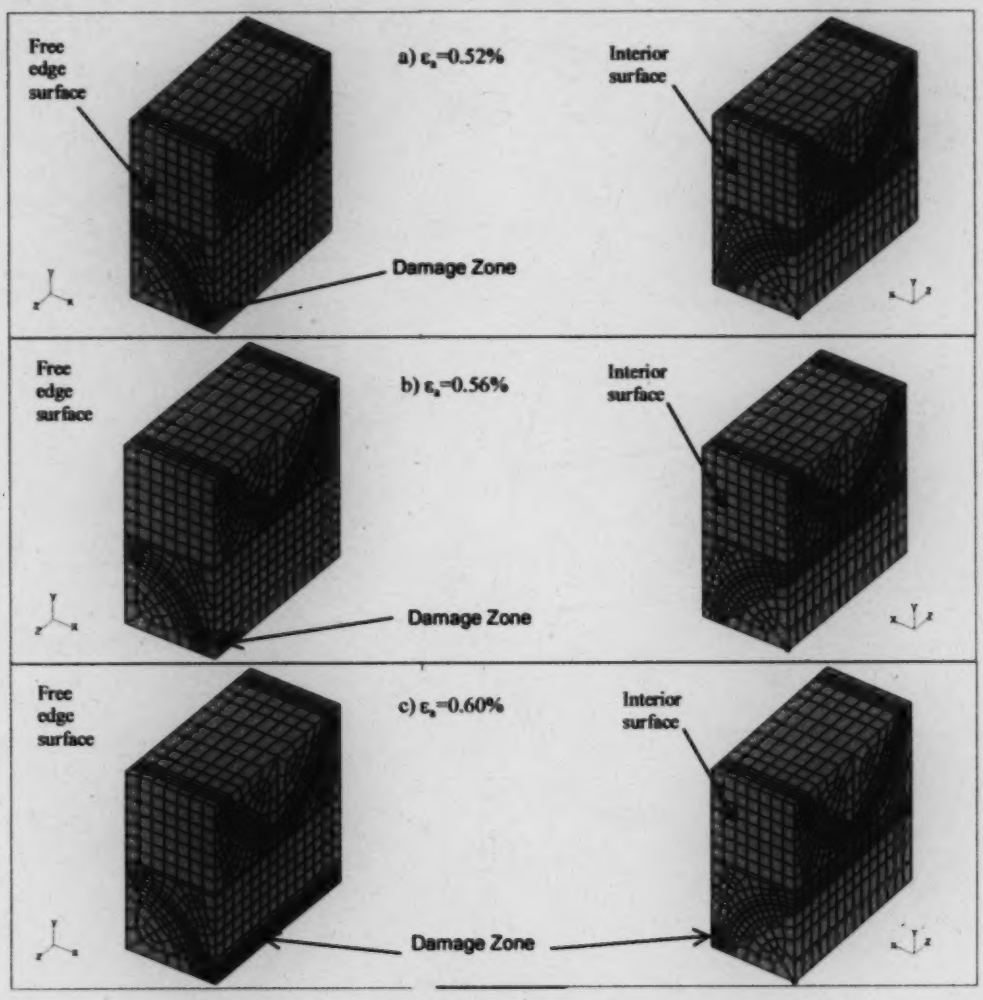

Figure 3.7 Prediction of damage initiation by the free edge model

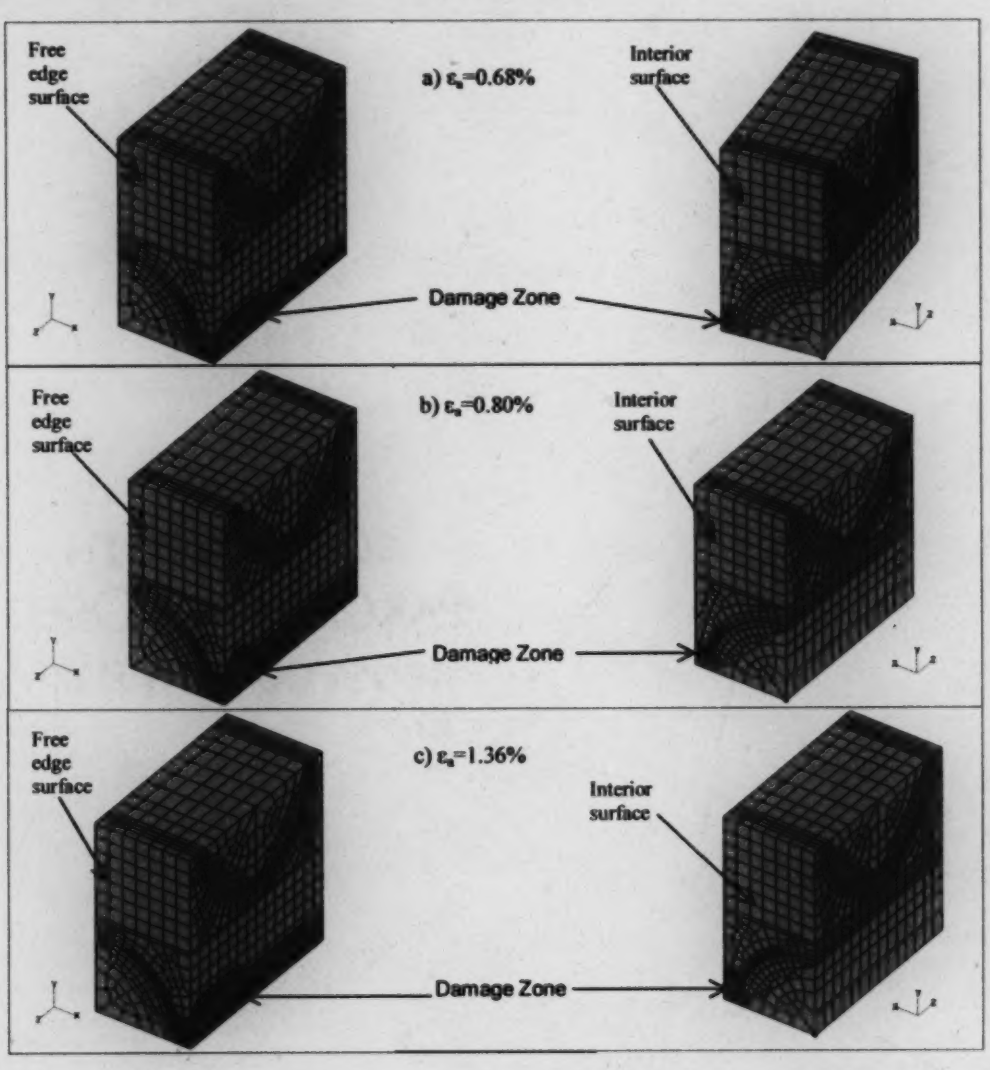

Figure 3.8 Prediction of damage propagation by the free edge model

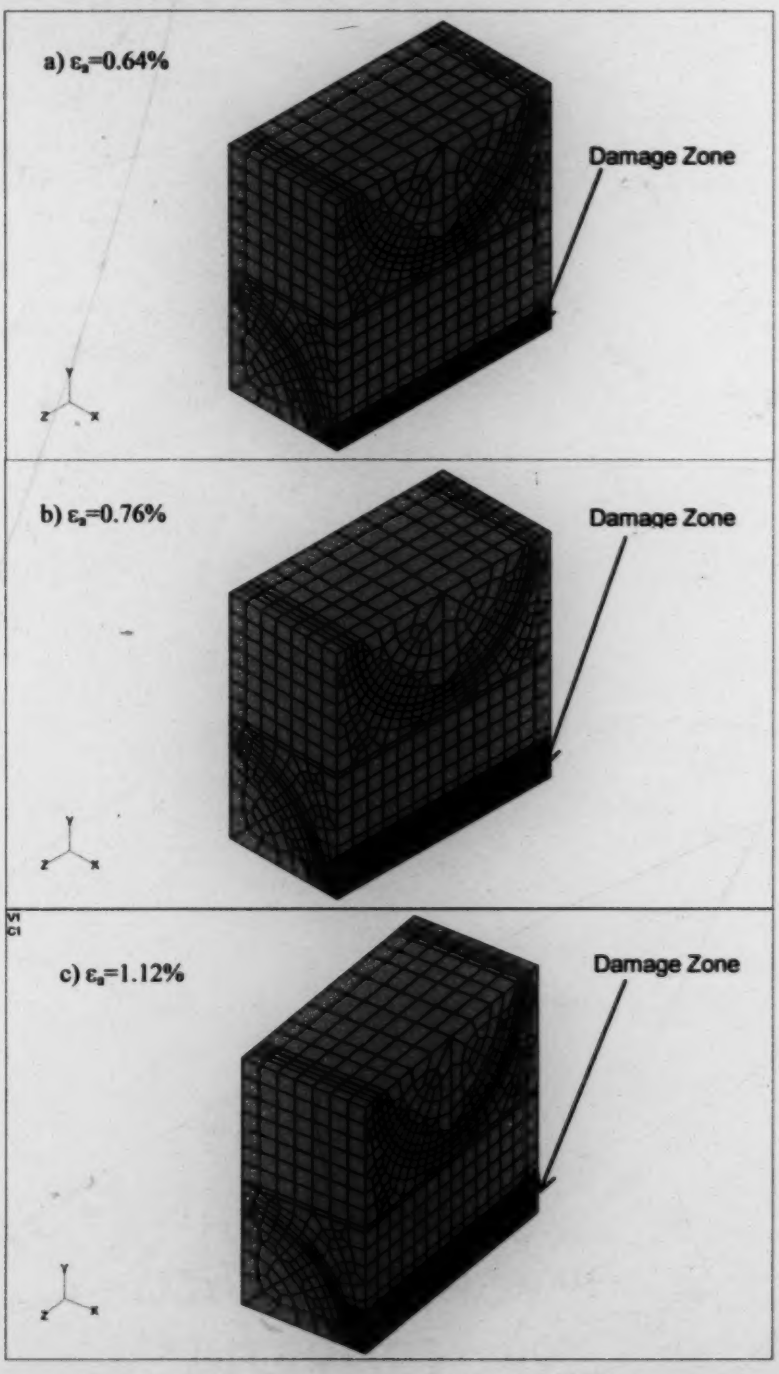

Figure 3.9 Prediction of damage propagation by the interior RVE model

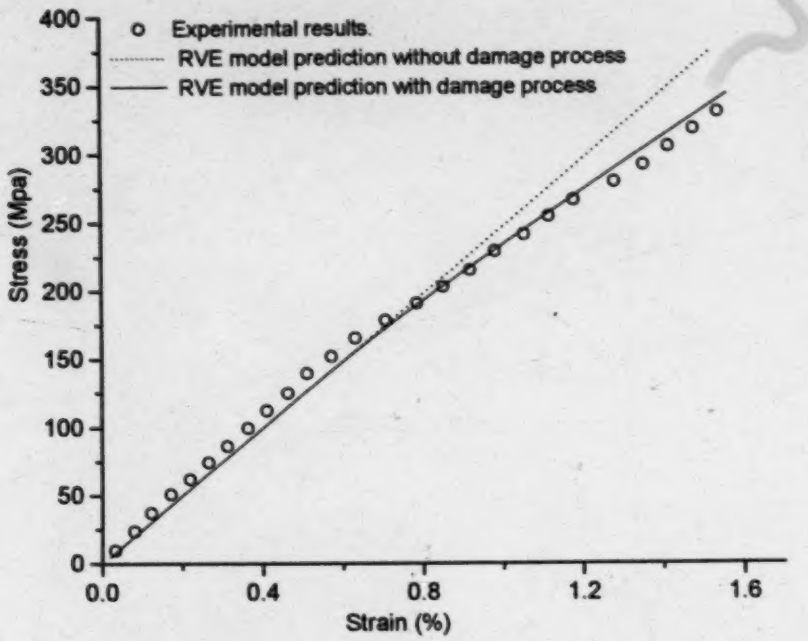

Figure 3.10 Prediction of stress-strain response of $[0/90]_{ns}$ laminate by the interior RVE model

Bibliography

1. Tsai, S.W. and Hahn, H.T., " Introduction to Composite Laminates", Technomic Publishing Co., Inc., Lanchaster, PA, 1980.
2. Caslini, M., Zanotti, C., and O'Brien, T.K., "Study of Matrix Cracking and Delamination in Glass/Epoxy Laminates", *Journal of Composites Technology & Research*, Vol.9, 1987, pp.121-130.
3. Cherkaoui, M., Muller, D., Sabar, H., and Berveiller, M., "Thermoelastic Behavior of Composites with Coated Reinforcements: A Micromechanical Approach and Applications. *"Computational Materials Science"*, Vol.5, 1996, pp45-52.

4. Zhu, H. and Sankar, B.V., "Evaluation of Failure Criteria for Fiber Composite Using Finite Element Micromechanics", *Journal of Composite Materials*, Vol.32, 1998, pp766-782.

5. Li, D.S. and Wisnom, M.R., "Finite Element Micromechanical Modeling of Unidirectional Fiber-reinforced Metal-matrix Composites", *Composites Science and Technology*, Vol.51, 1994, pp545-563.

6. Sherwood, J.A. and Quimby, H.M., "Micromechanical Modeling of Damage Growth in Titanium Based Metal-matrix Composites", *Computers and Structures*, Vol. 56, 1995, pp505-514.

7. Allen, D.H., Jones, R.H. and Boyd, J.G. "Micromechanical Analysis of A Continuous Fiber Metal-matrix Composite Including the Effects of Matrix Viscoplasticity and Evolving Damage", *Journal of Mechanics and Physics of Solids*, Vol.42, 1994, pp505-529.

8. Kwon, Y.W. and Berner, J.M., "Micromechanics Model for Damage and Failure Analysis of Laminated Fibrous Composites", *Engineering Fracture Mechanics*, Vol.52, 1995, pp231-244.

9. Tandon, GP, Kim, RY and Dutton RE, "Micromechanical Edge Effects in Glass Matrix Composites", *Proceedings of the ASME Aerospace and Materials Divisions*, AD. Vol. 51, 1996, American Society of Mechanical Engineers, New York, N.Y., pp 61-75.

10. Xia, Z. and Ellyin, F., "Time-dependent behavior and viscoelastic constitutive modeling of an epoxy polymer", *Polymers & Polymer Composites*, Vol.6, 1998, pp75-83.

11. Chen, W.H. and Huang, T.F. "Three Dimensional Interlaminal Stress Analysis at Free edge of Composite Laminate", *Computers & Structures*, Vol.32, 1982, pp1275-1286.

12. Lee, J.D. "Three Dimensional Finite Element Analysis of Damage Accumulation in Composite Laminate", *Computer & Structures*, Vol.32, 1982, pp335-350.

13. Chang, C.C., Sandhu, R.S., Sierakowski, R.L. and Wolfe, W.E. "Continuous Strain Finite Element Analysis of Free Edge Effect in Laminated Composite Specimens", *Journal of Composites Technology & Research*, Vol.10, 1988, pp.54-64.

14. Wanthal, S.P. and Yang H.T.Y., "Three Dimensional Finite Element Formulations for Laminate Plates", *Journal of Reinforced Plastics and Composites*, Vol.10, 1991, p330-354.

15. Chen, Y., Xia, Z. and Ellyin, F. "A Viscoelastic Micro-mechanical Analysis of Thermal Residual Stress Evolution in Glass Fiber/Epoxy Cross-ply laminates" *Submitted to Journal of Composite Materials*, 1999

16. ADINA, User Manual 1984, ADINA Engineering Inc. Watertown, MA.

17. Garrett, K.W. and Bailey, J.E., "Multiple Transverse Fraction in 90 Cross-ply Laminates of a Glass Fiber-Reinforced Polyester", *Journal of Materials Science*, Vol.12, 1977, pp157-168.

18. Parvizi, A., Garret, K.W. and Bailey, J.E., "Constrained Cracking in Glass Fiber-Reinforced Epoxy Cross-Ply Laminates", *Journal of Materials Science*, Vol.13, 1978, pp195-201.

19. Hoover, J.W., Kujawski, D. and Ellyin, F. "Transverse cracking in symmetric and unsymmetric glass fiber/epoxy matrix laminates," *Composite Science and Technology*, Vol.57, 1997, pp1513-1526.

20. Kurtz, R.D., Pagano N.J., "Analysis of the deformation of a symmetrically-loaded fiber embedded in a matrix material. *Composites Engineering*, Vol.1, 1991, pp13-27.

21. Crossman, F.W. and Wang, A.S.D., "The Dependence of Transverse Cracking and Delamination on Ply Thickness in Graphite/Epoxy Laminates", *Damage in Composite Materials, ASTM, STP 775*, American Society for Testing and Materials, Philadelphia, PA, 1982, pp118-139

22. Wang, A.S.D., Slomiana, M. and Bucinell, R.B. "Delamination Crack Growth in Composite Laminates", *Delamination and Debonding of Materials, ASTM STP 876*, American Society for Testing and Materials, Philadelphia, PA, 1985, pp136-167.

Chapter 4

A Viscoelastic Micro-mechanical Analysis of Thermal Residual Stress Evolution in Glass Fiber/Epoxy Cross-ply Laminates

4.1 Introduction

When polymer composites are cooled from their fabrication temperature to room temperature, thermal residual stresses are generated inside the composites due to the mismatch in the coefficient of thermal expansion (CTE) of the fiber and matrix constituents. Because of the viscoelastic nature of the epoxy matrix, however, these residual stresses will decrease through a process of stress relaxation. In general, experimental methods in measuring the evolution of these residual stresses are complicated and the results rather difficult to interpret [1]. Consequently, to understand the features of these processing-induced residual stresses, one has to rely primarily on analytical and/or numerical methods.

The use of micromechanical modeling of composites in terms of their constituent properties is a common numerical tool for investigating thermal stress state on the micro-scale. This method provides detailed stress and deformation fields on the microscopic scale as well as the prediction of effective mechanical properties, especially when viscoelastic mechanisms are involved [2]. Generally, the build-up of residual stresses in micromechanical models involves two processes: generation and relaxation. The generation of residual stresses depends on the difference between the

Young's moduli and CTE of the fiber and matrix materials, and on the consolidation temperature. The relaxation, on the other hand, is a function of the time-dependent inelastic properties of the matrix. A number of investigations [3-7] have used a micromechanical model to study the generation of residual stresses in metal matrix composites but, only a few researchers [8-9] have extended this methodology to polymer-based composites. To the best of our knowledge, a micromechanical model, including both generation and relaxation, has not been used to study the evolution of residual stresses in glass fiber/epoxy laminates. It is the goal of this work to address these issues.

In this study, a three-dimensional micromechanical model is used in a viscoelastic finite element analysis to investigate the evolution of thermal residual stresses in a thick [0/90] glass fiber/epoxy cross-ply laminate. The model, with the appropriate boundary condition, predicts thermal stresses and displacements both near and away from the free edge surface. The effect of the free edge surface on the generation of residual stresses is contrasted with that of the interior. Three different cooling rates have been selected to examine the role of matrix viscoelasticity in the generation of residual stresses, the dimensional changes and the subsequent relaxation behavior. The analysis incorporates a nonlinear viscoelastic constitutive relation [10] particularly suited for the epoxy matrix. This constitutive model has been implemented into the finite element analysis code, ADINA [11], through the user-defined subroutine. In addition, the effective thermal expansion coefficient of the cross-ply laminate is shown to be generally time-dependent. For the sake of comparison, the results for a unidirectional laminate of the same material with the same volume fraction are also presented.

4.2 Micromechanical modeling

The accuracy of a micromechanical model depends on the choice of model, which usually incorporates various geometrical and material assumptions. Typically, in a micromechanical model, it is assumed that the fibers are uniformly dispersed with the same cross section in composite and packed in a square array. Consequently, only one identical representative volume element (RVE), much smaller than the whole composite laminate, is required to be analyzed by the finite element method.

4.2.1 Finite element representation

Figure 4.1 shows a micromechanical representation of a thick cross-ply [0/90] laminate. The lay-up structure of the laminate in Fig.4.1 is fully periodic in all three directions. Each unidirectional layer could be represented by a unit cube with a single fiber having the same fiber volume fraction as the ply. The RVE is representative of a typical internal array of the composite that is not influenced by edge effects. Due to the symmetry conditions, only 1/8 of the RVE needs to be analyzed by the finite element method. In the analysis to follow, the fiber volume fraction was taken to be 52.5%, and is the same for each layer in the laminate.

The effect of the free edge surface for the cross-ply laminate is also studied by selecting a RVE near the free edge surface of laminate as shown in Fig.4.2. Numerical tests by micromechanical model have shown that the free edge effect is localized near the edge surface with a maximum length less than half of the fiber diameter. Therefore, the edge effect on the interior surface, one fiber diameter away from the free edge

surface, is negligible. Consequently, symmetry conditions would still apply to the interior surface and here also only 1/8 of this RVE needs to be analyzed.

Moreover, in the present study, a unidirectional laminate, similar to the one used in Ref 7, with the same volume fraction has been modeled. All RVE models were meshed using a three-dimensional, eight-node hexahedral element. Figure 4.3 shows the finite element mesh and dimensions for the unidirectional model (Fig.4.3a), cross-ply [0/90] model (Fig.4.3b) and free edge model (Fig.4.3c). A very thin, finely meshed layer was used in the vicinity of the interface, where significant stress gradients may occur. A convergence study was carried out based on the assumption that further refinement in mesh resolution did not result in appreciable changes in the contours of thermal stress and displacement fields. The current mesh substantially reduced the computation time during the relaxation analysis and yet remained relatively accurate in comparison to a further refined mesh.

4.2.2 Applied boundary conditions

Symmetric conditions were applied to the three finite element models on boundary surfaces X=0, Y=0 and Z=0, i.e.:

$$u(0, Y, Z) = 0 \tag{4.1}$$

$$v(X, 0, Z) = 0 \tag{4.2}$$

$$w(X, Y, 0) = 0 \tag{4.3}$$

The boundary conditions applied on surfaces X=1, Y=1 and Z=0.25 of the finite element model (Fig.4.2a) will enforce periodicity along all directions, i.e.

$$u(1, Y, Z) = u(1,0,0) \tag{4.4}$$

$$v(X, 1, Z) = v(0,1,0) \tag{4.5}$$

$$w(X, Y, 0.25) = w(0,0,0.25) \tag{4.6}$$

Identical periodic boundary conditions are also applied on surfaces X=1, Y=2 and Z=1 of the finite element model shown in Fig.4.2b, i.e.

$$u(1, Y, Z) = u(1,0,0) \tag{4.7}$$

$$v(X,2, Z) = v(0,2,0) \tag{4.8}$$

$$w(X, Y,1) = w(0,0,1) \tag{4.9}$$

Under these boundary conditions, each plane surface remains plane during deformation, but is free to displace in its own plane. A perfect bond between the fiber and matrix is assumed in the analysis.

In general, the free edge surface may not remain flat and it could have a slope discontinuity or distortion during the loading. For this case, the free surface (X=2) in Fig.4.3c was modeled as a traction free surface (that is, no constraints were imposed). Hence, periodic boundary conditions were only applied on the surfaces Y=2 and Z=1 of the finite element model shown in Fig.4.3c, i.e.

$$v(X,2, Z) = v(0,2,0) \tag{4.10}$$

$$w(X, Y,1) = w(0,0,1) \tag{4.11}$$

4.2.3 Material models for the fiber and epoxy matrix

In this study, the matrix is assumed to be a viscoelastic property determined by a given set of material parameters. These material constants are assumed to be independent of temperature.

The glass fiber is assumed to remain linear elastic, and is thus modeled by the generalized Hooke's law, with E=72.5 GPa, v=0.22 and CTE=5×10^{-6}/°C. The epoxy

matrix is modeled by a nonlinear viscoelastic constitutive relation recently developed by Xia and Ellyin. A complete version of the viscoelastic constitutive model is provided in Ref. [10] and here, for the sake of completeness, only a brief description will be given.

For the *uniaxial* stress state, the model can be represented by a finite number of nonlinear Kelvin elements and a spring element, connected in series as shown in Fig.4.4. The constitutive equations, generalized to the multiaxial stress state, are summarized below:

$$\{\dot{\varepsilon}_t\} = \{\dot{\varepsilon}_e\} + \{\dot{\varepsilon}_c\} \tag{4.12}$$

$$\{\dot{\varepsilon}_c\} = \sum_{i=1}^{n} \left(a_i [A] \sigma_{eq}^{\alpha_i - 1} \{\sigma\} - b_i \{\varepsilon_{ci}\} \right) \tag{4.13}$$

$$\{\dot{\sigma}\} = E[A]^{-1} \{\dot{\varepsilon}_e\} \tag{4.14}$$

In the above, $\{\dot{\varepsilon}_t\}$, $\{\dot{\varepsilon}_e\}$, $\{\dot{\varepsilon}_c\}$, $\{\dot{\sigma}\}$ are the total strain-rate, elastic strain-rate, creep strain-rate and stress-rate vectors (six components), respectively. The matrix [A] is given by:

$$[A] = \begin{bmatrix} 1 & -\nu & -\nu & 0 & 0 & 0 \\ -\nu & 1 & -\nu & 0 & 0 & 0 \\ -\nu & -\nu & 1 & 0 & 0 & 0 \\ 0 & 0 & 0 & 1+\nu & 0 & 0 \\ 0 & 0 & 0 & 0 & 1+\nu & 0 \\ 0 & 0 & 0 & 0 & 0 & 1+\nu \end{bmatrix} \tag{4.15}$$

which is related to the value of Poisson's ratio. It is to be noted that instead of a linear relation between $\{\dot{\varepsilon}_c\}$ and $\{\sigma\}$, a power function relation is introduced through the

stress factor $\sigma_{eq}^{\alpha_i - 1}$ in equation (13), where $\sigma_{eq} = (\frac{3}{2} s_{ij} s_{ij})^{1/2}$ is the von Mises equivalent stress and $s_{ij} = \sigma_{ij} - \frac{1}{3}\delta_{ij}\sigma_{kk}$ is the deviatoric stress tensor.

Although any number of Kelvin elements can be chosen, it is shown in Ref. [10] that two elements are sufficient. Based on test results, the material constants defined in equations (13) and (14) for the epoxy matrix were determined as follows:

$$a_1 = 5\times10^{-8}(\text{MPa})^{-2}, \quad \alpha_1 = 2, \; b_1 = 0.01,$$
$$a_2 = 1\times10^{-8}(\text{MPa})^{-2}, \quad \alpha_2 = 1, \; b_2 = 1\times10^{-6},$$
$$E = 2600\,\text{MPa}, \; \nu = 0.4 \text{ and } \text{CTE} = 63\times10^{-6}/^{\circ}\text{C}$$

The above viscoelastic material model has been implemented into the ADINA program through a user-supplied material model subroutine [11].

4.2.4 Implementation of thermal analysis in the model

In the present study, the thermal stresses induced during cooling from the fabrication temperature, T_f=149°C [12] to room temperature, T_r=23°C, are investigated. The fabrication temperature is regarded as a reference temperature at which the laminate is taken to be stress free in both the matrix and the fiber. A uniform spatial temperature throughout the model is assumed, i.e., the temperature of each node is specified to be identical at any time and to be varied at the same change rate of temperature. To show the effect of cooling rates on the residual stresses in the cross-ply laminate, the cooling process is simulated by applying incremental temperature drops at three different cooling rates of 126°C/min, 1.4°C/min, 0.15°C/min, respectively. The relaxation is simulated by dropping the laminate temperature from the fabrication

temperature to room temperature and then holding the laminate at room temperature for a long period.

4.3 Results and Discussion

The results of the finite element analysis for the generation and relaxation of residual stresses are presented in the form of stress contour plots for fiber and matrix materials in the following section. Stress components shown in this section are longitudinal and transverse stresses, respectively.

4.3.1 Residual stresses in fiber/epoxy laminates

The residual stresses induced by cooling from the stress free temperature of 149°C to 23°C at a rate of 1.4°C/min are shown for both the unidirectional and cross-ply laminates in Figs.4.5 and 4.6. The difference in the residual stress states between the unidirectional and the cross-ply are clearly demonstrated in both the longitudinal (σ_{zz}) and transverse (σ_{xx}) directions. For the unidirectional model, the longitudinal stress values range from a tensile value of 26.64 MPa in the matrix near the interface to a compressive value of 19.13 MPa in the fiber. These stresses are distributed symmetrically along the diagonal line of the model. The transverse stress, however, has no such symmetrical distribution. The maximum tensile stress occurs in the matrix with a value of 20.84 MPa near the interface and the maximum compressive stress occurred in the fiber near the interface zone on the top of the fiber with a value of 19.08 MPa.

In the case of cross-ply laminate (Fig.4.6), the longitudinal and the transverse stresses are very similar in distribution and magnitude. The stress values range from a tensile value of 42.27 MPa in the matrix near the interface to a compressive value of 76.49 MPa in the fiber.

As seen in these figures, while the longitudinal and transverse stresses show similar trends in magnitude and distribution for the cross-ply laminate, these stresses are different in the unidirectional laminate. Furthermore, the maximum tensile stress and compressive stresses in the cross-ply laminate are much higher than those in the unidirectional laminate. These differences between the two-laminate lay-ups indicate that the residual stresses in any ply of laminate are influenced significantly by the adjacent ply with different configurations. Different angle-ply laminates would have different residual stresses in both magnitudes and distributions.

4.3.2 Free Surface effect on residual stress of cross-ply laminate

To quantify the effect of the free edge surface, the residual stresses generated at a cooling rate of 126°C/min for the cross-ply laminate at and away from the free edge surface are compared in Figure 4.7. The deformation of the RVE model near the free surface is also shown in Fig.4.7. The transverse stresses are similar to those of the longitudinal stresses in both the magnitude and distribution for cross-ply laminates, as mentioned before. Therefore, in the analysis to follow, only the longitudinal stress (σ_{zz}) contours are given for the cross-ply laminate. It is seen from the figure that the tensile stresses in the free edge model are significantly different from those in the interior. Higher maximum tensile stresses occur in the 90° fiber at the free surface (61.33Mpa).

These stresses are much higher than the ones in the interior of laminate, which occur near the interface in the 0° fibers (48.13Mpa). However, the compressive stresses of the free edge were less different from those in the interior in both the magnitude and distribution. In addition, due to the free surface boundary condition used in the free edge model, the free edge surface does not remain plane after cooling to the room temperature. A residual distortion occurs on the free surface.

4.3.3 Stress relaxation of the cross-ply laminate

It was mentioned in section 2 that the generation of residual stresses in the current cross-ply model is governed by the viscoelastic nature of the epoxy matrix. Relaxation and creep may occur simultaneously during the cooling process. Hence, three different cooling rates were selected to study the time-dependent effect on the evolution of residual stresses in the cross-ply laminate. To illustrate the effect of viscous behavior of the matrix on the evolution of residual stresses in the cross-ply laminate, the result of a purely elastic matrix material representation with the same RVE model, is also presented. The residual stress contours in the longitudinal direction for a cooling rate of 0.15°C/min, along with the purely elastic solution, are shown in Figure 4.8. The elastic solution is obtained by assuming $\{\dot{\varepsilon}_c\}=0$ in equation (12) and (13). A comparison of Figs.4.6, 4.7 and 4.8 shows that the elastic solution predicts the highest tensile and compressive residual thermal stress than that obtained by a viscoelastic solution. The magnitudes of the maximum tensile and compressive stresses in the cross-ply laminate under a faster cooling rate are greater than those under a slower cooling rate (Fig.4.10).

These suggest a strong effect of the matrix viscous behavior on the evolution of thermal residual stress. An elastic matrix model induced higher residual stresses in the cross-ply laminate than a viscoelastic matrix model irrespective of the rate of cooling.

The stress relaxation behaviors of the cross-ply laminate at three different cooling rates are numerically simulated herein. Once the laminate reaches room temperature, it is held at that temperature for a long period. Figure 4.9 depicts the residual stress contour in the longitudinal direction (σ_{zz}) for the cross-ply laminate cooled at a rate of 1.4°C/min and held at room temperature for 2133 minutes. When contrasting this figure with Fig.4.6, it can be clearly seen that the tensile and compressive residual stresses have decreased significantly in both the fiber and matrix zones. It should be noted that the results shown here exhibit a strictly mechanical effect due to viscous behavior of the epoxy and thermal mismatch between fiber and matrix. This point is illustrated more clearly in Fig.4.10. For the purpose of comparison, the relaxation evolution of the maximum tensile and compressive stresses for the cross-ply laminate at three different cooling rates as well as the elastic solution is shown in Fig.4.10.

It is seen that irrespective of the cooling rates, the residual stress tends to an asymptotic value with the passage of time. The cooling rate affects the initial (maximum) residual stress value. Hence, it is advisable to reduce the cooling rate as much as is practically possible so as to avoid matrix cracking when first reaching the ambient temperature. The residual stress within a purely elastic matrix, however, could not relax with the passage of time and remains constant. In order to illustrate time-dependent effect on the cross-ply dimensions, the evolution of the average shrinkage strain in the longitudinal direction is shown in Fig.4.11. Here, the average shrinkage

strain in the longitudinal direction is obtained from the following equation [13] based on the finite element model developed in section 2:

$$\overline{\varepsilon_L^s} = \frac{-w(0,0,1)}{L} \tag{4.16}$$

where L is the length of the RVE model in the Z direction. Again, it is noted that higher cooling rates results in a higher shrinkage strain when the laminate is cooled to the ambient temperature. The thermal shrinkage strain, however, tends to a small value over a long period when held at room temperature. It is seen that the time at which the change in slope becomes insignificant, is about 1800 minutes, see Fig.4.10 and 4.11. After this period, thermal residual stress and shrinkage strain tend toward a limiting value. The above results indicate that, as long as no damage was initiated in the cross-ply laminate during the cooling process, there would be negligible difference in the final thermal residual stress and deformation for a cross-ply laminate when cooled at different rates and held at the ambient temperature for a long time.

4.3.4 Time effect on thermal expansion coefficient of viscoelastic composites

Unlike the CTE of elastic composites and time-independent elastic-plastic composites discussed in Ref. [14], the viscoelastic matrix characteristic to creep and to relax implies that the CTE of the viscoelastic composite will, in general, not remain constant but will be a function of time for a certain period. In this section, the time effect on the thermal expansion coefficient of viscoelastic composites will be examined for both unidirectional and cross-ply laminates.

In the present study, the CTE of the viscoelastic composite is defined as:

$$\alpha = \frac{\bar{\varepsilon}}{\Delta T} \tag{4.17}$$

where $\bar{\varepsilon}$ is the average shrinkage strain in a given direction and ΔT is the uniform temperature change from the fabrication temperature to room temperature. As stated earlier, because of the relaxation, the shrinkage strain changes with time after the laminate is cooled to the room temperature. Therefore, although the CTE values of the constituents are specified material parameters, it is apparent that the composite CTE as defined above becomes a derived quantity and varies with time, due to the mechanical constraint imposed on the viscous matrix.

Since the average shrinkage strains for the cross-ply laminate in the longitudinal and transverse directions are equal, there is only one CTE for the cross-ply laminate, defined as α_C. The longitudinal and transverse CTE for the unidirectional laminate are labelled α_u^L, α_u^T, respectively. Figures 4.12 and 4.13 show the change of CTE as a function of time for unidirectional and cross-ply laminates, separately. The CTE values calculated by the elastic solution are also shown in these figures. The average shrinkage strain is measured after the laminate is cooled to room temperature at a cooling rate of 1.4°C/min. The time-dependence of CTE due to the viscoelastic composite is clearly seen to be quite pronounced in these figures. Over a long period (~2000 minutes), the CTE of composite tends to reach a constant value.

The CTE of the composite predicted by the current model can be compared with analytical solutions. For isotropic elastic composites, the CTE can be expressed as [15]:

$$\alpha_u^L = \frac{E_m \alpha_m V_m + E_f \alpha_f V_f}{E_m V_m + E_f V_f} \tag{4.18}$$

where α_u^L is the CTE of the composite in the longitudinal direction, E_m and E_f are the elastic moduli, α_m and α_f are the CTE, and V_m and V_f are volume fraction of the matrix and fibers, respectively. This equation, proposed by Schapery, is widely used to predict the longitudinal composite CTE from the properties of the constituents. Schapery [15] has also presented the solution for the transverse CTE of unidirectional composite as:

$$\alpha_u^T = \alpha_m V_m (1+\upsilon_m) + \alpha_f V_f (1+\upsilon_f) - \alpha_u^L \upsilon_C \tag{4.19}$$

where ν_m, ν_f, and ν_c are the Poisson's ratio of the matrix, fibre and composite, respectively. The longitudinal and the transverse CTE of unidirectional composite calculated by equations (18) and (19) are 6.825×10^{-6}/°C and 42.11×10^{-6}/°C, respectively. The asymptotic values obtained from viscoelastic solution in Fig.4.12 are 5.21×10^{-6}/°C and 39.46×10^{-6}/°C, respectively. It is noted that the analytically predicted values are higher than the limiting viscoelastic values. Those predicted by eqs. (18) and (19) result in an overestimation by 31% and 7%, respectively. On the other hand, the analytically predicted values are in good agreement with the elastic solution shown in Fig.4.12. This is because both the analytical solution and elastic solution do not account for the time effect on the CTE of viscoelastic composites.

4.4 Conclusions

A nonlinear viscoelastic micromechanical analysis of the evolution of the thermal residual stresses in unidirectional and cross-ply laminates has been presented. The 3-D micromechanical model is capable of analyzing the variation of the stress/deformation states in the interior of the composite as well as near the free edge surface. This investigation shows that the viscous behavior of the matrix plays an important role in the evaluation of the residual stresses in composites. The following conclusion are drawn from the present study:

1. Different ply orientations generate different residual stresses in both magnitude and distribution.
2. Due to the effect of the free edge surface, there is a significant difference in the residual stresses both in the magnitude and in distribution between the interior surface and free surface of cross-ply laminates. Residual distortion also occurs near the free surface of cross-ply laminate.
3. A higher cooling rate results in higher initial residual stresses than a lower cooling rate. Hence, a higher cooling rate may lead to cracking of the epoxy matrix.
4. In the absence of damage initiation during the cooling process, the residual thermal stresses in the composite reduce to a small value over a long time irrespective of the effects of the different cooling rates.
5. The CTE value of the viscoelastic composite is significantly influenced by the viscous behavior of the matrix. It changes as a time function and tends to reach a limiting value over a long period (~2000 minutes).

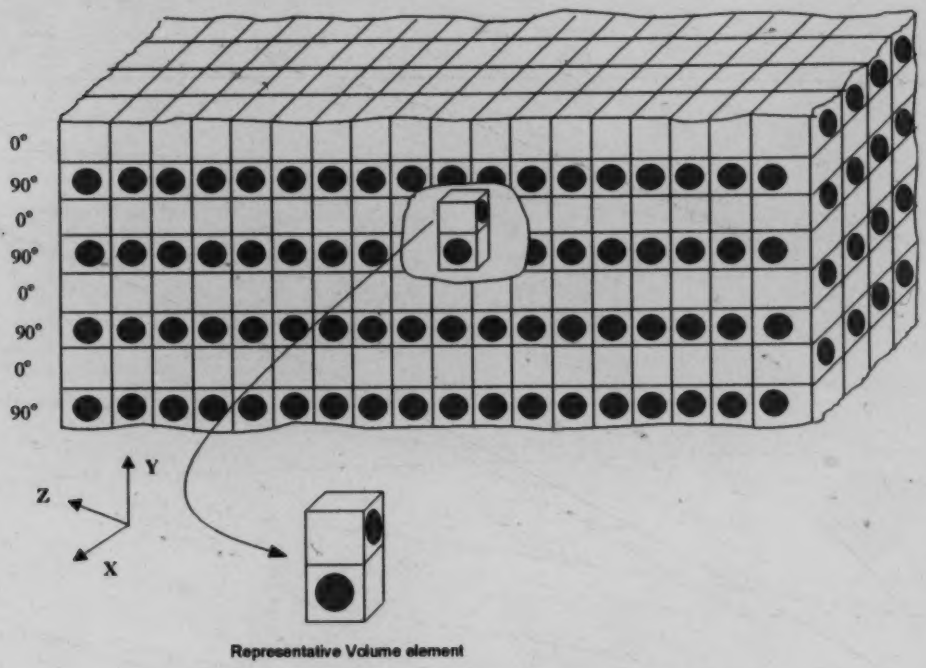

Figure 4.1 Representative Volume Element for [0/90] laminate

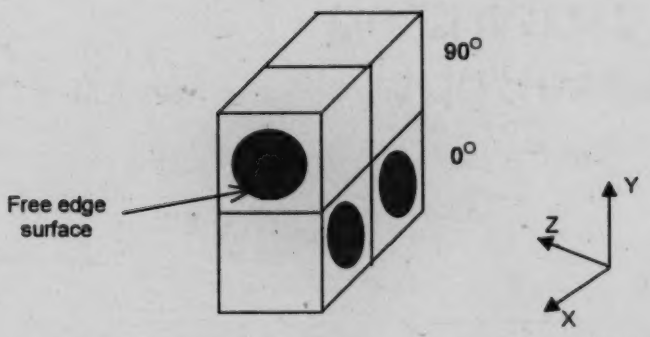

Figure 4.2. A RVE model near free edge surface for [0/90] laminate

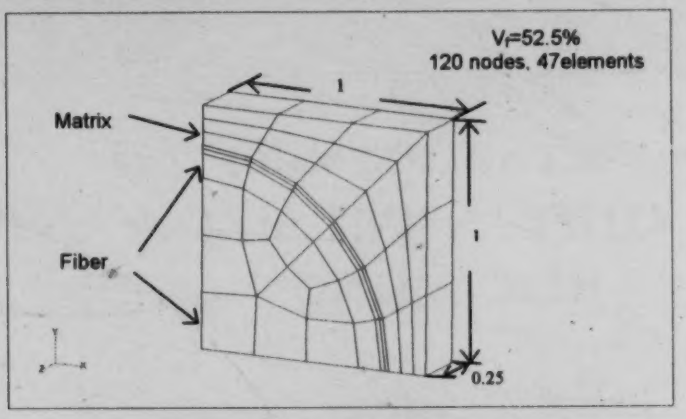

a) Three-dimensional finite element mesh of unidirectional laminate

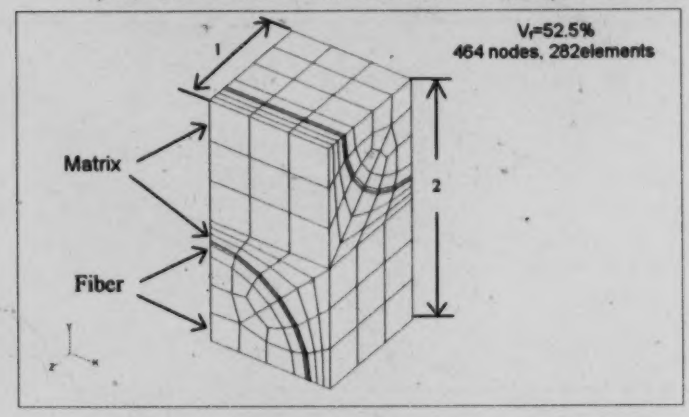

b) Three-dimensional finite element mesh of [0/90] laminate

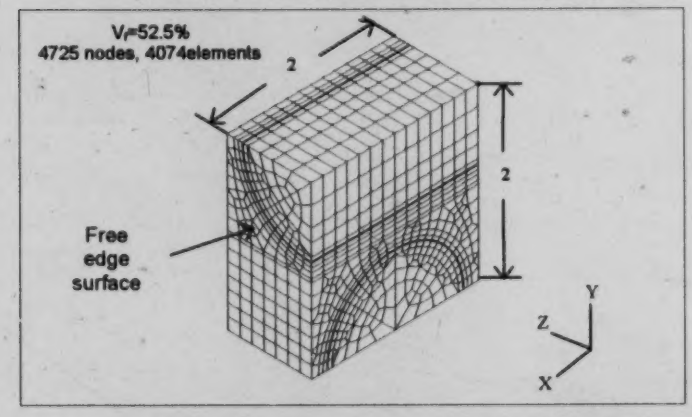

c) Three-dimensional finite element mesh of [0/90] laminate near free edge surface

Figure 4.3 The 3-D models and FEM meshing

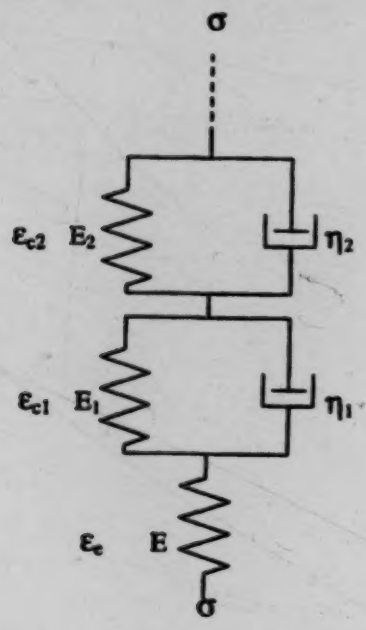

Figure 4.4. A viscoelastic model represented by a finite series of Kelvin elements coupled with an elastic spring

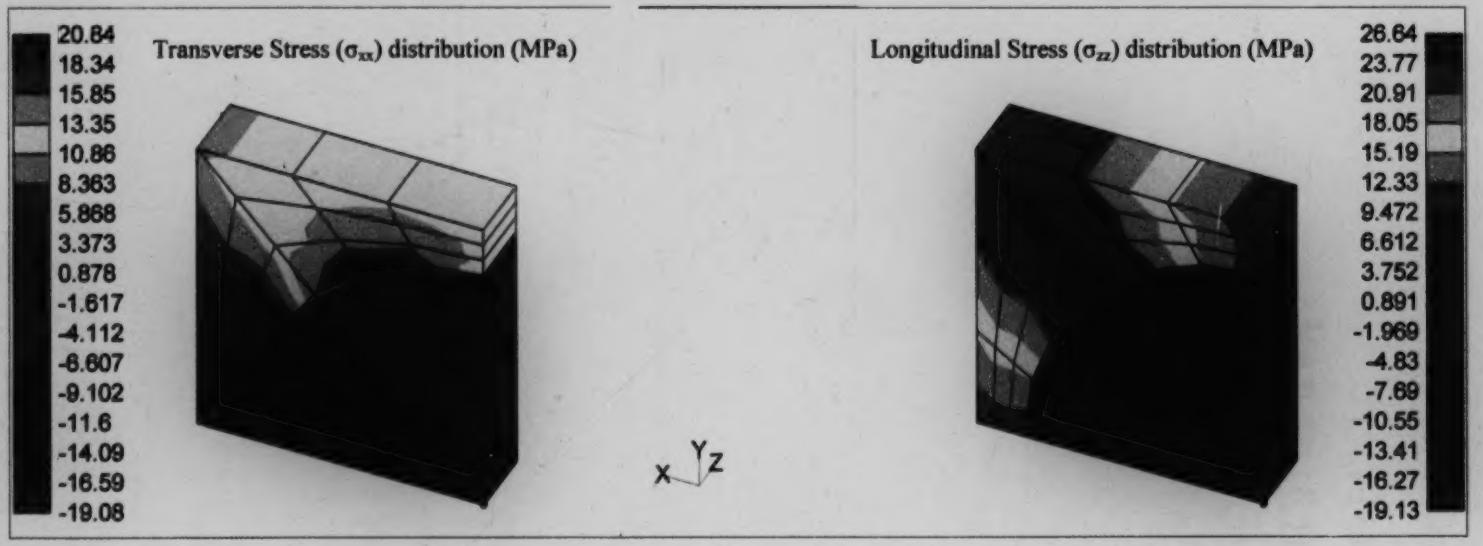

Figure 4.5 Residual stress distribution for unidirectional laminate at cooling rate of 1.4° C/min

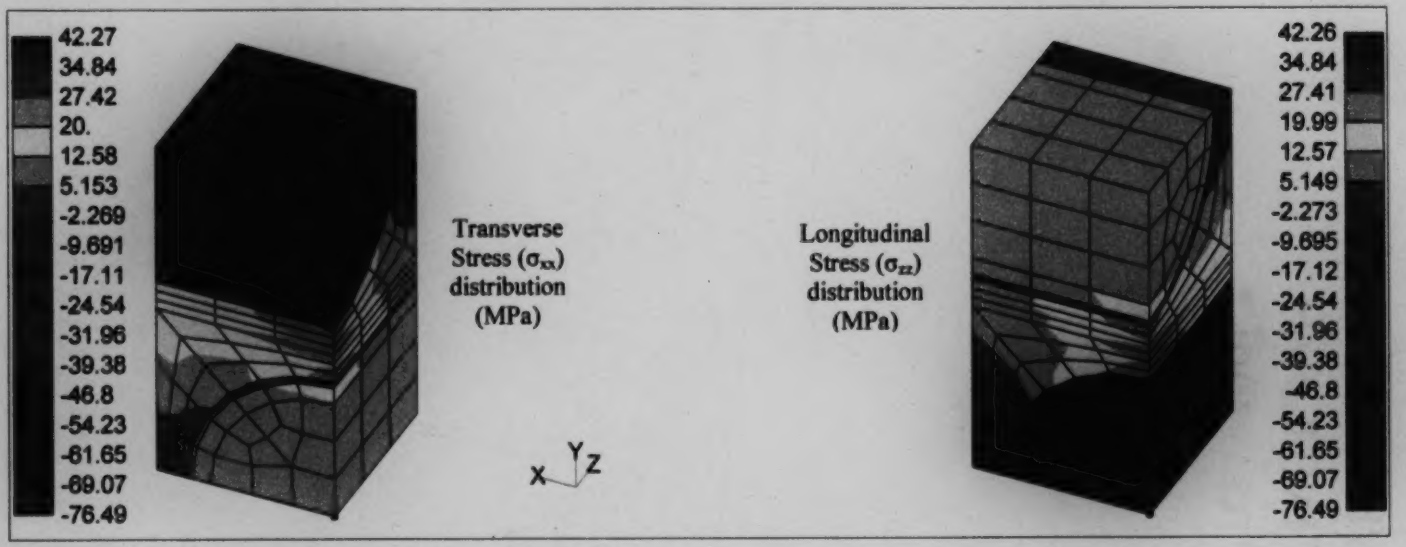

Figure 4.6 Residual stress distribution for cross-ply laminate at cooling rate of 1.4° C/min

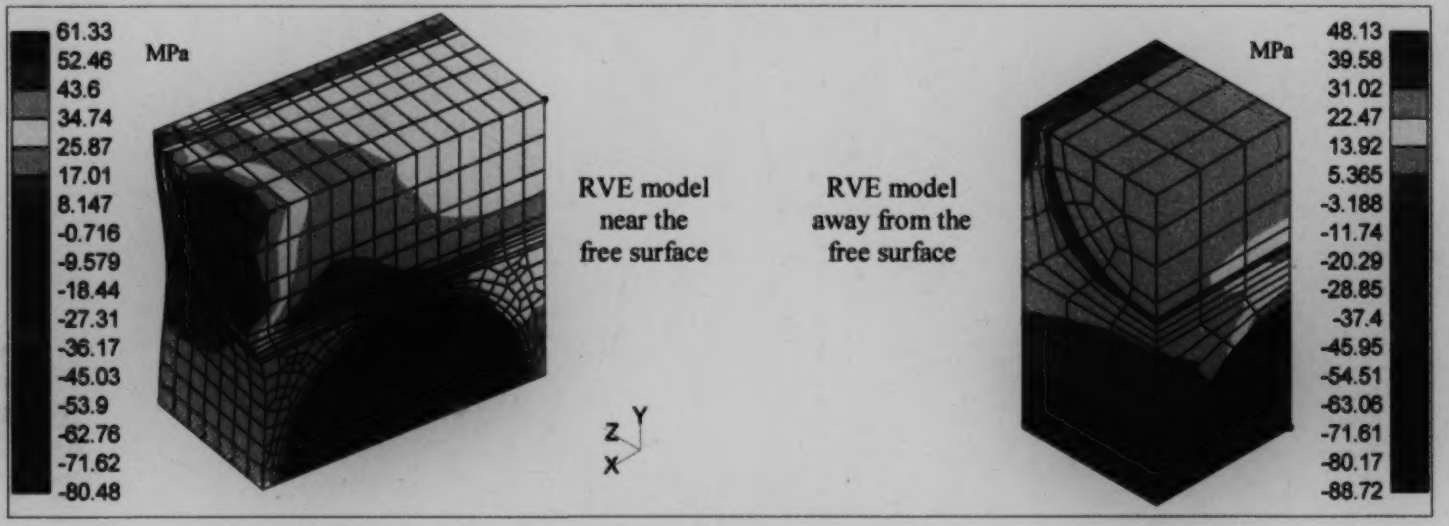

Figure 4.7 Thermal residual stresses distributions in longitudinal direction (σ_{zz}) for cross-ply laminate near and away from free edge surface at cooling rate of 126° C/min

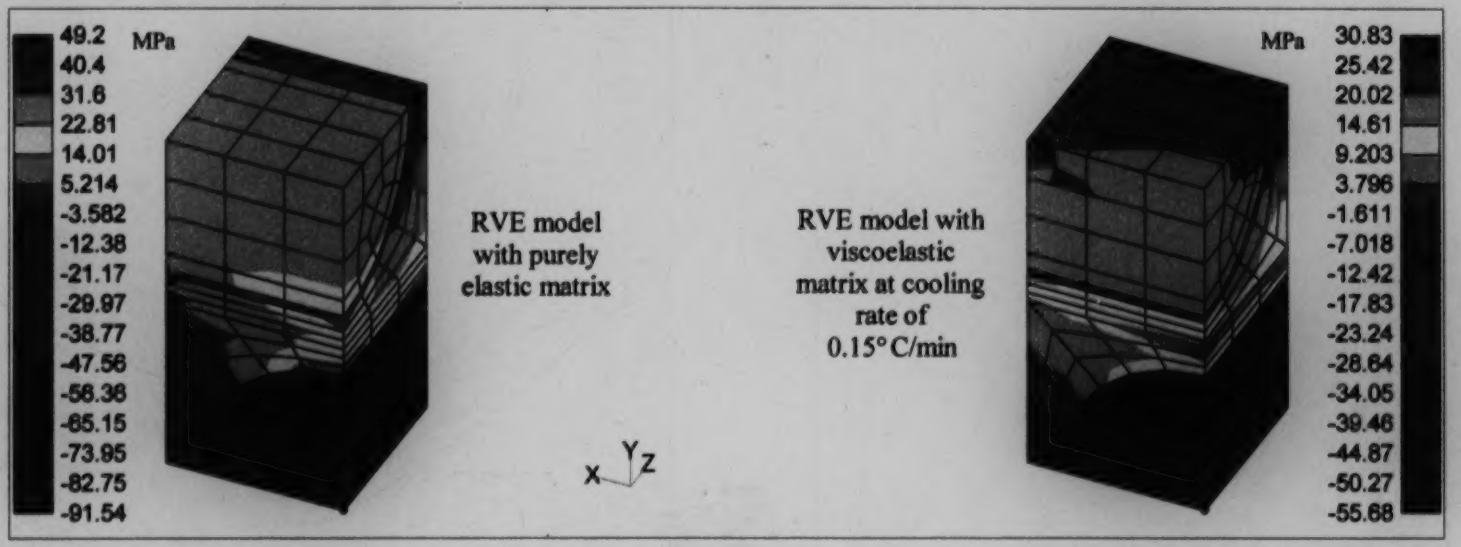

Figure 4.8 Thermal residual stresses distributions in longitudinal direction (σ_{zz}) for cross-ply laminate with two different matrix materials.

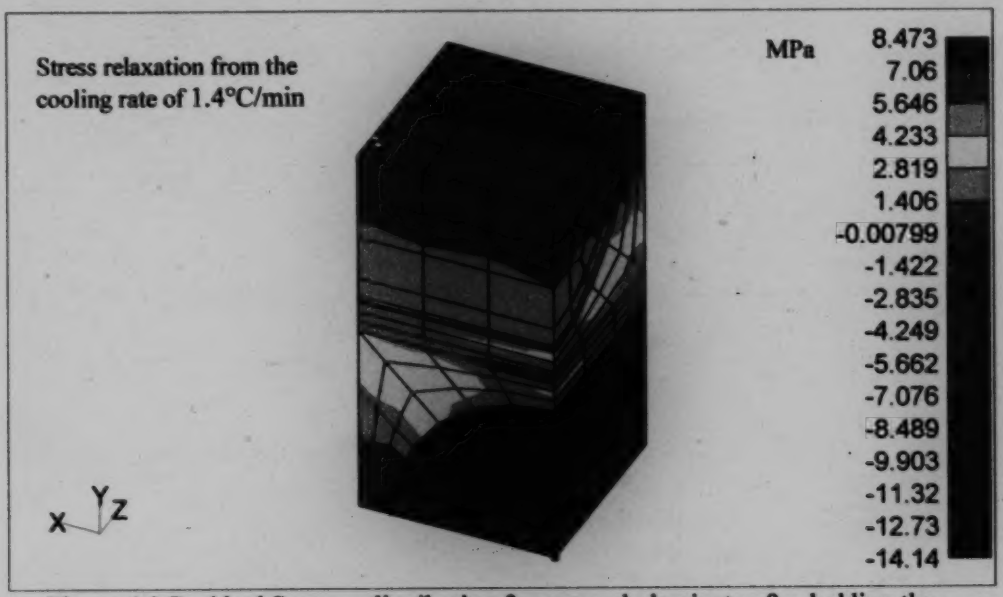

Figure 4.9 Residual Stresses distribution for cross-ply laminate after holding the model at room temperature for 2133 minutes.

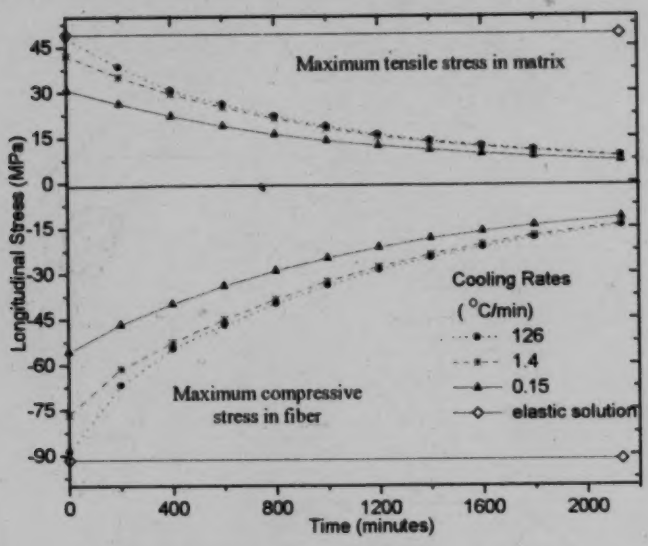

Figure 4.10 Residual stress relaxation in cross-ply model for different cooling rates

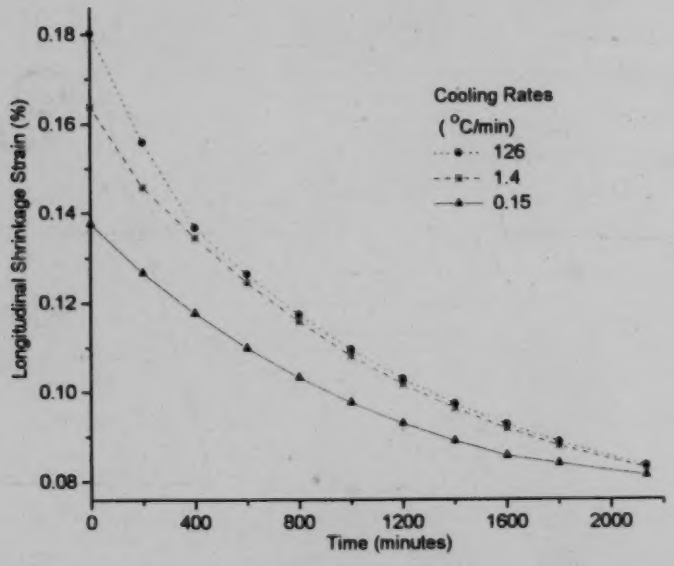

Figure 4.11 Strain recovery in cross-ply laminate for different cooling rates

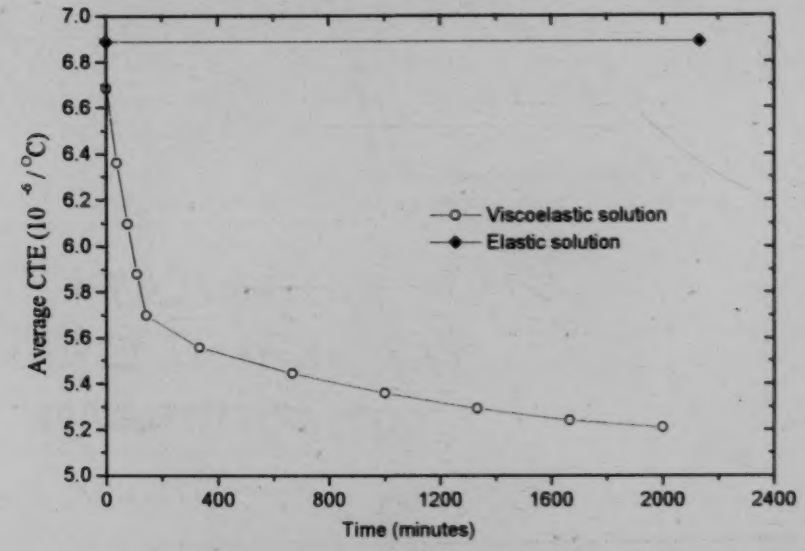

a) Average CTE values along the longitudinal direction of unidirectional model

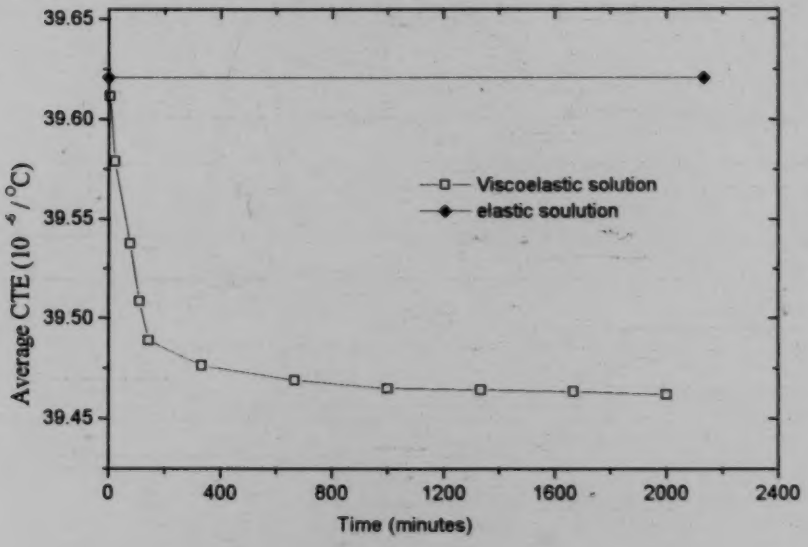

b) Average CTE values along the transverse direction of unidirectional model

Figure 4.12 Calculated average CTE of unidirectional composite

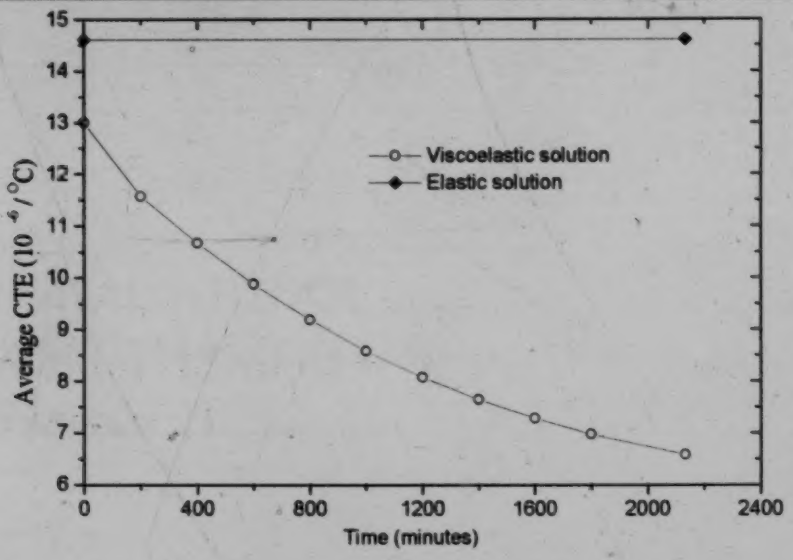

Figure 4.13 Calculated average CTE of cross-ply laminate as a function of time

Bibliography

1. Majumdar, S., Singh, J.P., Kupperman, S. D. and Krawitz, A., "Application of Neutron Diffraction of Measure Residual Strains in Various Engineering Composite Materials," *ASME Journal of Engineering Materials and Technology*, Vol.113, No.1, 1991, pp.51-58.
2. M.Chaturvedi and Y-L. Shen, "Thermal Expansion of Particle-Filled Plastic Encapsulant: A Micromechanical Characterization," *Acta mater.* Vol. 46, No.12, 1998, pp.4287-4302.
3. Nimmer, R. P. "Fiber-Matrix Interface Effect in Presence of Thermally Induced Residual Stresses," *Journal of Composite Technology & Research*, Vol. 12, No.2, 1990, pp.65-75.
4. Wisnom, M. R. "Factors Affecting the Transverse Tensile Strength of Unidirectional Continuous Silicon Carbide Fiber Reinforced 6061 Aluminum," *Journal of Composite Materials*, Vol.24, No.7, 1990, pp.706-726.

5. Rangaswamy, P. and Jayaraman, N. "Residual Stresses in SCS-6/Ti-24Al-11Nb Composite: Part II-Finite Element Modeling," *Journal of Composite Technology & Research*, Vol. 16, No.1, 1994, pp.54-67.

6. Chandra, N., Ananth, C. R. and Garmestani, H., "Micromechanical Modeling of Process-Induced Residual Stresses in Ti-24AlNb/SCS Composites," *Journal of Composite Technology & Research*, Vol.16, No.1, 1994, pp.37-46.

7. Bigelow, C. A., "Thermal Residual Stresses in Silicon-Carbide/Titanium [0/90] Laminate," *Journal of Composite Technology & Research*, Vol.15, No.4, 1993, pp.304-310.

8. Gardner, S. D. Pittman, C. U. and Hackett, R.M., "Residual Thermal Stresses in Filamentary Polymer-matrix Composites Containing An Elastomeric interphase," *Journal of Composite Materials*, Vol.27, No.8, 1993, pp.830-860.

9. Sung Yi, "Effect of a time-dependent interfacial layer on the thermo-mechanical response of polymer matrix composites", *Journal of Materials Processing Technology*, Vol.67, 1997, pp.183-188.

10. Xia, Z. and Ellyin, F., "Time-dependent behavior and viscoelastic constitutive modeling of an epoxy polymer", *Polymers & Polymer Composites*, Vol.6, 1998, pp75-83.

11. ADINA, User Manuel 1984, ADINA Engineering Inc. Watertown, MA.

12. Hoover, J.W., "Transverse Cracking of $[\pm\theta,90_3]_S$ Composite Laminates", M. Sc. Thesis, Department of Mechanical Engineering, University of Alberta, 1999.

13. Sun, C.T., and Vaidya, R.S., "Prediction of composite properties from a representative volume element," *Composite Science and Technology*, Vol.56 1996, pp.171-179.

14. Hull, D., "An Introduction to Composite Materials", Cambridge Solid State Science Series, G.B. , 1981.

15. Schapery, R. A., "Thermal Expansion Coefficients of Composite Materials Based on Energy Principles", *Journal of Composite Material*, Vol. 2, 1968, pp.380.

Chapter 5

Conclusions

The primary goal of this study was to model the mechanical behavior and damage process of glass fiber/epoxy cross-ply laminates under uniaxial loads using a three-dimensional finite element analysis. The comprehensive micromechanical model includes the effect of viscoelasticity of the matrix and the consideration of thermal residual stress in cross-ply laminates, as well as incorporating appropriate damage criteria to predict the damage initiation and propagation inside the composite. The results presented here have led to the following conclusions:

1. This investigation has shown that to perform an effective micro-mechanical analysis and to obtain reliable predictive results, the following three prerequisite conditions must be fulfilled:

a) The RVE model must correctly represent the lay-up geometry of the laminates as well as the original volume fraction for each layer and the proportion of layers with different fiber orientations.

b) The constitutive models must be able to accurately represent the constituents' behaviors. A generalized Hookes' law is usually sufficient for the fibers. But for the polymer matrix materials, a nonlinear viscoelastic constitutive models is required

c) A proper damage criterion and a post-damage constitutive relation to simulate the damage process should also be introduced in the model. The values of damage parameters must be based on realistic experimental observations

2. The multi-layer unit cell models developed in this study provide a accurate representation of the laminate lay-up structure of cross-ply laminates. These models enable the finite element analysis to generate detailed distribution of stress/strain in the matrix and fiber, which are essential for understanding the damage mechanisms. With proper damage criteria introduced for the matrix and interface, the damage initiation and propagation observed in the experimental investigations are predicted by the micromechanical model. In addition, the model predicted global stress-strain response was in good agreement with the experiment observation of the cross-ply laminates

3. In laminates, damage generally initiates at the free surface, and propagates into the interior of the cross-ply laminate. The crack initiates at a lower global strain on the free edge surface compared with that at the interior zone. Although early damage initiation occurs near the fiber/matrix interface near the free edge surface, the transverse matrix cracking, which initiates later on, first propagates into the interior of the cross-ply laminate. The early damage initiation on the free edge surface, however, has negligible effect on the global mechanical properties of the cross-ply laminate.

4. The nonlinear viscoelastic constitutive model introduced in the micromechanical analysis plays an important role in the evaluation of the residual stresses in composites. A high cooling rate results in the higher initial residual stresses than that of a low cooling rate. Hence, it is feasible that a higher cooling rate may lead

to cracking of the epoxy matrix. However, in the absence of damage initiation during the cooling process, the residual thermal stresses in the composite reduce to a small value with passage of time, irrespective of the different cooling rates. The thermal residual stress also causes a distortion in the free edge area of the laminates.